Izmir Institute of Technology

Department of Mechanical Engineering ME404 Final Report

Eren Meydan-280203050

Gamze Uyaroğlu-280203076

Spring 2026

ABSTRACT

This study investigates the effect of phase change material (PCM) domain geometry on the thermal performance of latent heat thermal energy storage systems intended for solar thermal applications. Five storage tank configurations were designed, manufactured from transparent plexiglass, and experimentally tested using RT42 paraffin as the PCM. All geometries were built with an approximately constant PCM volume of about 1 L, so that the observed performance differences could be attributed mainly to tube position and heat transfer surface area rather than to the storage material.

Charging and discharging experiments were carried out using water as the heat transfer fluid at 65 °C and a flow rate of 2.14 L/min, and the temperature evolution within the PCM domain was recorded using K-type thermocouples. The results showed that lowering the tube toward the bottom of the tank (eccentric placement) enlarges the PCM region above the heat source, increases the Rayleigh number, and strengthens buoyancy-driven natural convection, leading to faster and more uniform melting during charging. In contrast, the centered configurations provided shorter and more symmetric conduction paths, resulting in more balanced solidification during discharging.

Increasing the heat transfer area through a second tube or through fins further improved the charging performance by reducing the conduction-limited regions of the PCM domain. Overall, no single geometry was optimal for both processes, and the obtained results provide a basis for the planned integration of the optimized storage unit with a parabolic dish solar collector.

ÖZET

Bu çalışma, güneş enerjisi uygulamalarına yönelik gizli ısı termal enerji depolama sistemlerinde faz değişim malzemesi (PCM) domain geometrisinin termal performans üzerindeki etkisini incelemektedir. Beş farklı depolama tankı konfigürasyonu tasarlanmış, şeffaf pleksiglastan üretilmiş ve PCM olarak RT42 parafin kullanılarak deneysel olarak test edilmiştir. Tüm geometrilerde yaklaşık 1 L sabit PCM hacmi kullanılmıştır; böylece gözlemlenen performans farklılıklarının depolama malzemesinden ziyade temel olarak boru konumu ve ısı transfer yüzey alanından kaynaklanması sağlanmıştır.

Şarj ve deşarj deneyleri, ısı transfer akışkanı olarak 65 °C sıcaklıktaki su ve 2.14 L/dk debi kullanılarak gerçekleştirilmiş; PCM domaini içerisindeki sıcaklık değişimi K-tipi termokupllar ile kaydedilmiştir. Sonuçlar, borunun tankın alt kısmına doğru konumlandırılmasının, yani eksantrik yerleşimin, ısı kaynağının üstündeki PCM bölgesini genişlettiğini, Rayleigh sayısını artırdığını ve kaldırma kuvveti etkili doğal taşınımı güçlendirdiğini göstermiştir. Bu durum, şarj sürecinde daha hızlı ve daha homojen bir erimeye yol açmıştır. Buna karşılık, merkezde konumlandırılmış geometriler daha kısa ve daha simetrik iletim yolları sağlayarak deşarj sürecinde daha dengeli bir katılaşma davranışı oluşturmuştur.

İkinci bir boru veya kanatçıklar aracılığıyla ısı transfer alanının artırılması, PCM domainindeki iletimle sınırlı bölgeleri azaltarak şarj performansını daha da iyileştirmiştir. Genel olarak, her iki süreç için de tek bir geometri en uygun çözüm olarak öne çıkmamıştır; ancak elde edilen sonuçlar, optimize edilmiş depolama ünitesinin parabolik çanak tipi güneş kolektörü ile planlanan entegrasyonu için bir temel oluşturmaktadır.

TABLE OF CONTENTS

LIST OF FIGURES

LIST OF TABLES

INTRODUCTION

1.1.1 Thermal Energy Storage System

The rising global energy demand and environmental concerns with fossil fuel use have accelerated the transition to renewable energy technologies. Among the renewable energy sources, solar energy has attracted great attention because of its abundance, sustainability and low environmental impact. However, the intermittent nature of solar radiation creates a mismatch between energy generation and energy demand, making energy storage systems essential for the efficient utilization of renewable energy resources.

Thermal Energy Storage (TES) systems are able to store thermal energy when there is a surplus of energy and release it when needed. TES technologies improve system reliability, increase the energy efficiency and help overcome the intermittency problems associated with renewable energy systems. These systems are widely used in solar thermal applications, industrial waste heat recovery, district heating and concentrated solar power systems.[1]

TES systems can be divided in three main categories; sensible, latent and thermochemical energy storage. Sensible heat storage is based on temperature changes in a storage medium such as water, rocks or molten salts. This method is simple and cheap, but in general requires large storage volumes. Latent heat storage uses phase change materials (PCMs) that absorb and release significant amounts of thermal energy as they change from solid to liquid and back again. Latent heat storage has a much higher energy storage density and an almost constant operating temperature during the phase transition process compared with sensible heat storage.[2] Thermochemical energy storage stores energy in reversible chemical reactions and has the highest theoretical storage density of all TES technologies. But its practical implementation is often limited by system complexity and cost.

One of the most promising technologies for solar thermal energy storage applications is PCM-based latent heat storage systems due to their high storage capacity and compatibility with renewable energy applications.

1.1.2 Phase Change Materials in Thermal Energy Storage

Phase Change Materials (PCMs) are thermal energy storage materials that store and release energy through phase transitions, typically between solid and liquid states. Unlike sensible heat storage materials, which store energy by changing temperature, PCMs utilize latent heat during melting and solidification processes. This characteristic allows large amounts of thermal energy to be stored within a relatively small volume.

During the charging process, thermal energy supplied to the PCM increases its temperature until the melting point is reached. Once melting begins, the material absorbs a significant amount of energy while maintaining a nearly constant temperature. During the discharging process, the stored energy is released as the PCM solidifies. This ability to store thermal energy at an almost constant temperature makes PCMs highly attractive for thermal management and energy storage applications.

PCMs are generally classified into three categories: organic, inorganic, and eutectic materials. Organic PCMs, such as paraffin-based materials, exhibit good chemical stability and reliable cycling performance. Inorganic PCMs, including salt hydrates and molten salts, often provide higher thermal conductivity and latent heat capacity but may experience phase segregation and supercooling. Eutectic PCMs combine two or more materials to achieve specific melting temperatures and thermal properties.

The main advantages of PCM-based thermal energy storage systems include high energy storage density, reduced storage volume, and nearly isothermal charging and discharging processes. These characteristics improve the efficiency and stability of thermal energy storage systems, particularly in solar thermal applications.

Despite these advantages, several challenges remain. Most PCMs possess relatively low thermal conductivity, which slows heat transfer and increases charging and discharging times. In addition, leakage during the liquid phase may occur if proper containment systems are not implemented. For this reason, various enhancement techniques such as fins, metal foams, nanoparticles, and geometry optimization have been investigated to improve PCM thermal performance.

In this study, four different PCMs representing both low-temperature and high-temperature thermal energy storage applications were considered: RT42, Coral Cornet 159A, Erythritol, and Solar Salt. These materials were selected to investigate the influence of PCM domain geometry under different operating temperature ranges and potential solar thermal energy storage applications.

1.1.3 Geometry Effect on PCM Performance

The thermal performance of PCM-based thermal energy storage systems is dependent on the thermophysical properties of PCM and the geometry of the storage domain. Heat is conducted into the material during melting. As the liquid PCM layer increases, natural convection becomes more and more dominant and plays an important role in temperature distribution and melting behavior.

The geometry of the PCM domain directly influences the formation of natural convection currents in the storage system. The flow patterns during melting can be affected by parameters such as aspect ratio, PCM layer thickness, enclosure dimensions, arrangement of heat transfer surface etc. Hence, for the same PCM and operating conditions, different geometries may have different melting rates, charging times and thermal efficiencies.

Multiple studies have shown that the performance of latent heat thermal energy storage systems can be significantly improved by geometry optimization. Rectangular enclosures are one of the most studied configurations due to their simple design and ease of manufacturing. Previous studies showed that the change of the dimensions of the PCM domain influences the distance between the heat transfer surface and the PCM, thereby affecting the heat transfer rates and the development of the melting front. Also, fins or tubes can be used to increase the heat transfer area, thereby reducing the melting time and improving the temperature uniformity inside the storage medium. [3,4]

Therefore, geometry optimization has been an effective way to improve the performance of PCM without any modification of the storage material itself. The present study is based on this concept, in which the effect of various PCM domain shapes on melting behavior and charging performance is studied with the same PCM volume. The goal is to determine the optimal geometry for future applications in thermal energy storage and solar integration.

1.1.4 Solar Integration of PCM Systems

In recent years, the integration of phase change materials (PCMs) with solar thermal systems has attracted much attention due to the capability of PCMs to store excess thermal energy and release it when needed. The thermal energy storage systems can be combined with the solar technologies to improve the system reliability and partially overcome the intermittency problem of the solar energy.

Among the solar thermal technologies able to reach relatively high temperatures is the parabolic dish collector, which focuses solar radiation to a focal point. This makes them suitable for medium and high temperature thermal energy storage applications with PCMs such as erythritol and solar salt.[1]

The second phase of the study was solar integration in this project. The most effective storage configuration will be evaluated for integration with a parabolic dish collector after conducting experimental studies of different PCM domain geometries under controlled laboratory conditions. This approach is meant to evaluate the suitability of the optimized PCM storage system for future solar thermal energy storage applications.

1.2 Aim and Objectives

The aim of this project is to investigate the effect of PCM domain geometry on the thermal performance of latent thermal energy storage systems and to determine the most effective configuration for future solar thermal energy storage applications.

To achieve this aim, different PCM storage geometries were designed, manufactured, and experimentally evaluated under controlled operating conditions. The influence of geometry on melting behavior, temperature distribution, and charging performance was analyzed while maintaining a constant PCM volume. Furthermore, both low-temperature and high-temperature phase change materials were considered to assess the applicability of the proposed designs over a wide operating temperature range.

The main objectives of the project are summarized as follows:

- To design and manufacture different PCM storage geometries.
- To experimentally investigate the melting behavior of phase change materials.
- To compare the charging performance of different PCM domains.
- To evaluate the effect of geometry on heat transfer and melting front development.
- To determine the optimum PCM domain configuration.
- To investigate the suitability of different PCM materials for thermal energy storage applications.

- To evaluate the potential integration of the optimized storage system with a parabolic solar collector.
- To contribute to the development of efficient latent thermal energy storage systems for future solar energy applications.

1.3 Design Criteria

The thermal energy storage system was designed according to the following criteria:

- Maintaining a constant PCM volume for all tested geometries to ensure a fair performance comparison.
- Maximizing heat transfer between the heat transfer fluid (HTF) and the PCM.
- Reducing charging time by promoting effective heat distribution within the PCM domain.
- Enhancing natural convection during the melting process.
- Achieving a more uniform melting front development throughout the storage domain.
- Minimizing the distance between the heat transfer surface and the PCM.
- Providing compatibility with different PCM types operating at low and high temperatures.
- Ensuring reliable temperature measurement through appropriate thermocouple placement.
- Preventing PCM leakage during repeated melting and solidification cycles.
- Maintaining structural integrity of the storage tank under operating conditions.
- Using materials that are readily available and economically feasible.
- Allowing easy manufacturing, assembly, and modification of different geometric configurations.
- Providing compatibility with future solar thermal integration.
- Ensuring safe and repeatable experimental operation.

1.4 Limiting Factors

The design and experimental evaluation of the thermal energy storage system were subject to several technical, financial, and operational limitations:

- Limited project budget for materials, instrumentation, and prototype development.
- Availability and procurement difficulties of certain PCM materials, particularly high-temperature PCMs.
- Manufacturing limitations associated with plexiglass machining and assembly.
- Potential leakage issues at joints, fittings, and sealing interfaces during repeated melting and solidification cycles.
- Limited thermal conductivity of PCM materials, resulting in longer charging and discharging times.
- Temperature measurement uncertainty associated with thermocouple accuracy and sensor positioning.
- Limited number of available measurement points despite using multiple thermocouples.
- Laboratory space and equipment availability constraints.
- Time limitations imposed by the project schedule and academic calendar.
- Difficulty in maintaining perfectly uniform operating conditions during experiments.
- Safety considerations when working with high-temperature PCMs and thermal oils.
- Weather dependency of the solar thermal system during outdoor testing.
- Limited access to solar radiation during unfavorable environmental conditions.
- Scale limitations of the experimental setup compared to industrial-scale thermal energy storage systems.
- Material property variations and uncertainties obtained from manufacturer datasheets and literature sources.

PROJECT MANAGEMENT

2.1 Work Breakdown Structure (WBS)

To ensure systematic execution, the project was divided into manageable sections. WBS encompasses all phases from initial literature review to the final reporting.

Table 1. WBS Table

WBS Code	Task Name	Description / Deliverable
1	**Project Management & Planning**	Definition of timeline, Gantt chart creation, and cost estimation.
2	**Literature Review & Conceptual Design**	Review of PCM melting behaviours, design alternatives, and final design selection.
3	**Manufacturing & Fabrication**	Sourcing materials (plexiglass, copper tubes, PCMs), tank fabrication, and tube integration.
4	**Experimental Setup & Commissioning**	Integration of HTF loop, parabolic collector setup, instrumentation, and calibration.
5	**Experimental Testing**	Parametric studies on geometry, flow rates, PCM materials, and high-temp solar-driven testing.
6	**Data Analysis & Reporting**	Data processing, performance evaluation, and compilation of the final project report.

2.2 Linear Responsibility Chart (LRC)

The project responsibilities were distributed equally between team members Gamze Uyaroğlu and Eren Meydan. The workload across all 5 presentation stages was evaluated, resulting in a perfectly balanced total work contribution of 250 points each (out of 500).

The table below outlines the primary (P) and secondary (S) responsibilities for key activities:

Table 2. LRC Table

Task / Activity	Gamze Uyaroğlu	Eren Meydan
1. Conceptual Design & Selection	Primary	Secondary
2. Manufacturing (Welding & Assembly)	Secondary	Primary

3. Sourcing Materials	Primary	Secondary
4. Experimental Setup Configuration	Secondary	Primary
5. Instrumentation & Calibration	Primary	Secondary
6. Conducting Parametric Experiments	Primary	Secondary
7. Solar Collector (High-Temp) Setup	Secondary	Primary
8. Data Acquisition & Recording	Primary	Secondary
9. Data Processing (Calculations)	Secondary	Primary
10. Final Report Writing	Secondary	Primary

2.3 Planned Gantt Chart

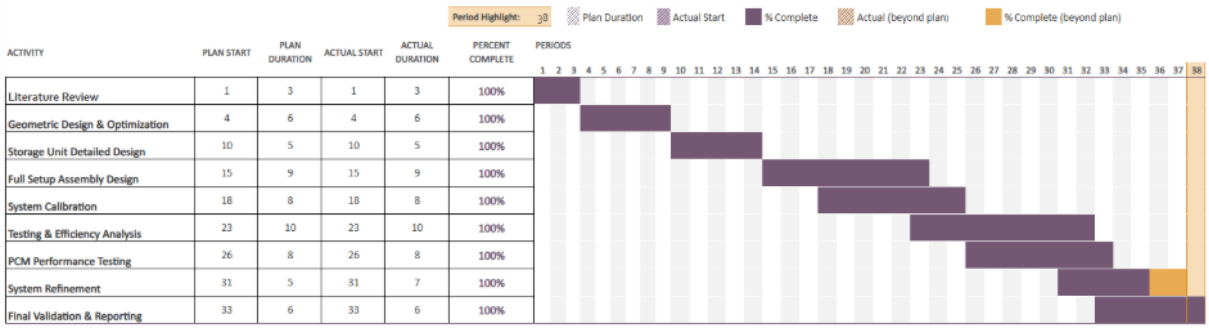
Period Highlight: 38
Plan Duration
Actual Start
% Complete
Actual (beyond plan)
% Complete (beyond plan)

ACTIVITY	PLAN START	PLAN DURATION	ACTUAL START	ACTUAL DURATION	PERCENT COMPLETE
Literature Review	1	3	1	3	100%
Geometric Design & Optimization	4	6	4	6	100%
Storage Unit Detailed Design	10	5	10	5	100%
Full Setup Assembly Design	15	9	15	9	100%
System Calibration	18	8	18	8	100%
Testing & Efficiency Analysis	23	10	23	10	100%
PCM Performance Testing	26	8	26	8	100%
System Refinement	31	5	31	7	100%
Final Validation & Reporting	33	6	33	6	100%

Figure 1. Gantt Chart

The project was completed within a time frame of 38 weeks, including all the main steps from literature review to final validation and reporting. The schedule was developed in a stepwise fashion so that each stage of the project could be built on the results of the previous stage. Particular attention was paid to design development, experimental installation construction, performance testing and evaluation of results. The proposed schedule of the project is shown in Figure 1. Excel format of the Gantt Chart is uploaded to the cloud folder.

2.4 Actual Project Timeline

The actual project execution generally followed the planned schedule. Most project activities were completed within their allocated timeframes, including the literature review, design development, system assembly, and experimental preparation stages. Minor deviations occurred during the refinement and validation phases due to additional design iterations and experimental adjustments. However, these changes did not significantly affect the overall project completion timeline. The most significant deviation occurred during the System Refinement phase, where additional testing and design modifications extended the duration from 5 weeks to 7 weeks.

2.5 Deviations and Delays

The single major deviation in the project schedule occurred during the transition to active testing, resulting in a 2-week delay. This was primarily caused by PCM leakage problems.

- **PCM Leakage:** When the PCM completely melted and transitioned to the liquid phase, its volume expanded, exerting pressure on the 3 mm plexiglass tank walls and joints. The initial sealing was insufficient, leading to leaks of the liquid PCM.
- **Tank Redesign & Manufacturing Revisions:** To solve this structural integrity issue without changing the domain geometry, immediate manufacturing revisions were required. The plexiglass joints had to be reinforced comprehensively.
- **Solution:** A specialized two-part epoxy adhesive was applied to the structural joints for mechanical strength, followed by a heavy application of high-temperature resistant silicone sealant to ensure absolute leak-tightness under thermal expansion.
- **Additional Testing:** Following the application of the new sealants, additional pressure and thermal cycling tests had to be conducted to ensure the system was robust enough for both low-temperature water circulation and high-temperature dielectric oil testing. This necessary troubleshooting accounted for the extended "System Refinement" period.

DESIGN STUDIES

This section presents the design process, engineering considerations, manufacturing details, and experimental evaluation of the subsystems developed within the scope of the project. The primary objective of the design studies was to investigate the effect of PCM domain geometry on the thermal performance of latent thermal energy storage systems while maintaining a constant PCM volume.

Different storage geometries were designed and manufactured to evaluate their influence on heat transfer, melting behaviour, and charging performance. In addition, the experimental setup, measurement system, and future solar integration components were developed to support both low-temperature and high-temperature thermal energy storage applications.

Each subsystem is presented separately, including its design criteria, conceptual design, engineering calculations, manufacturing and assembly process, and experimental evaluation.

3.1 Candidate Phase Change Materials

The selection of a suitable phase change material is one of the most important factors affecting the performance of latent thermal energy storage systems. Since the objective of this project is to investigate PCM domain geometry under different operating conditions, both low-temperature and high-temperature PCMs were considered.

Candidate materials were selected based on their melting temperature, latent heat storage capacity, availability, and suitability for thermal energy storage applications. Four different PCMs were investigated: RT42, Coral Cornet 159A, Erythritol, and Solar Salt.

RT42 and Coral Cornet 159A were selected as low-temperature PCMs due to their melting temperatures close to typical hot water operating conditions. Erythritol and Solar Salt were selected as high-temperature PCMs because of their suitability for concentrated solar thermal energy storage applications.

3.1.1 RT42

RT42 is an organic paraffin-based phase change material manufactured by Rubitherm GmbH. Due to its melting temperature range of 38–43 °C, RT42 is widely used in low-temperature thermal energy storage applications, including domestic hot water systems, building thermal management, and solar thermal energy storage.

One of the main advantages of RT42 is its relatively high latent heat storage capacity, which allows significant amounts of thermal energy to be stored within a narrow temperature range. In addition, RT42 exhibits good chemical stability, low corrosion potential, and reliable thermal cycling performance, making it suitable for repeated charging and discharging processes. [5]

RT42 was selected for this study as a representative low-temperature PCM. Its melting temperature is compatible with the operating conditions of the water-based experimental setup, allowing the investigation of PCM melting behavior and the influence of domain geometry under controlled laboratory conditions.

The main thermophysical properties of RT42 are presented in Table 3.

Table 3. The main thermophysical properties of RT42

Property	**Value**
PCM Type	Organic (Paraffin-based)
Melting Range	38–43 °C
Peak Melting Temperature	41 °C
Latent Heat Capacity	165 kJ/kg
Density (Solid)	880 kg/m³
Density (Liquid)	760 kg/m³
Specific Heat Capacity	2 kJ/kgK
Thermal Conductivity	0.2 W/mK

3.1.2 Coral Cornet 159A

Coral Cornet 159A is an organic phase change material developed for medium-temperature thermal energy storage applications. The material exhibits a phase change temperature of approximately 59 °C and operates within a temperature range of 52–62 °C. With a latent heat storage capacity of approximately 200 kJ/kg, Coral Cornet 159A provides higher temperature energy storage compared to RT42 while maintaining the advantages of organic PCMs.

The material was selected as an intermediate-temperature PCM to bridge the gap between low-temperature storage materials and high-temperature PCMs such as erythritol and solar salt. Its melting temperature is compatible with hot-water-based thermal storage systems and allows the investigation of PCM domain geometry under different thermal conditions.

In addition to its thermal storage capability, Coral Cornet 159A offers good thermal cycling stability and is designed for repeated melting and solidification processes. Therefore, it represents a suitable candidate for medium-temperature latent thermal energy storage applications. [6]

The main thermophysical properties of Coral Cornet 159A are presented in Table 4.

Table 4. The main thermophysical properties of Coral Cornet 159A

Property	Value
PCM Type	Organic PCM
Phase Change Temperature	~59 °C
Operating Temperature Range	52–62 °C
Latent Heat Capacity	~200 kJ/kg
Density	774 kg/m³ (@80 °C)
Kinematic Viscosity	4.4 mm²/s (@100 °C)
Solidification Temperature	>58 °C
Flash Point	>110 °C

3.1.3 Erythritol

Erythritol is an organic sugar alcohol that has attracted considerable attention as a high-temperature phase change material for thermal energy storage applications. Due to its high latent heat capacity and suitable melting temperature, erythritol is considered a promising candidate for solar thermal energy storage systems and medium-temperature energy storage applications.

The material exhibits a melting temperature of approximately 118 °C and a latent heat of fusion of 339.8 kJ/kg, which is significantly higher than many commercially available low-temperature PCMs. This high energy storage capacity enables a large amount of thermal energy to be stored within a relatively small volume. [3]

Erythritol was selected in this study as a representative high-temperature PCM for the second phase of the project, where solar thermal integration is considered. Its melting temperature is suitable for thermal energy supplied by a parabolic dish collector, making it a strong candidate for future solar thermal energy storage applications.

The main thermophysical properties of erythritol are presented in Table 5.

Table 5. The main thermophysical properties of erythritol

Property	**Value**
PCM Type	Organic PCM
Melting Temperature	117.7 °C
Solidus Temperature	116.7 °C
Latent Heat Capacity	339.8 kJ/kg
Density	1480 kg/m^3
Thermal Conductivity	0.326–0.733 W/m·K
Specific Heat Capacity (Solid)	1.38 kJ/kg·K
Specific Heat Capacity (Liquid)	2.76 kJ/kg·K
Dynamic Viscosity	2.77×10^{-5} – 0.023 kg/m·s
Thermal Expansion Coefficient	0.001014 K^{-1}

3.1.4 Solar Salt

Solar Salt is one of the most widely used thermal energy storage materials in concentrated solar power (CSP) systems. It is typically composed of a eutectic mixture of sodium nitrate ($NaNO_3$) and potassium nitrate (KNO_3), providing good thermal stability and suitability for high-temperature energy storage applications.

Compared to organic phase change materials, Solar Salt can operate at significantly higher temperatures, making it particularly attractive for solar thermal systems. Its relatively low cost, commercial availability, and extensive use in industrial thermal storage applications have made it one of the most studied materials for large-scale thermal energy storage.

In this study, Solar Salt was selected as a high-temperature storage material to evaluate the applicability of the proposed PCM domain geometries under elevated operating temperatures. In addition, its compatibility with concentrated solar thermal technologies makes it a suitable candidate for the future solar integration phase of the project.

The main thermophysical properties of Solar Salt are presented in Table 6.

Table 6. The main thermophysical properties of Solar Salt

Property	Value
PCM Type	Inorganic PCM
Composition	$NaNO_3$–KNO_3
Typical Composition	60 wt.% $NaNO_3$ / 40 wt.% KNO_3
Melting Temperature	~220 °C
Latent Heat Capacity	~110–170 kJ/kg*
Density	~1800–1900 kg/m³
Specific Heat Capacity	~1.5 kJ/kg·K
Thermal Conductivity	~0.5 W/m·K
Application	Concentrated Solar Power (CSP) and High-Temperature TES

Based on their thermophysical properties and operating temperature ranges, the selected PCMs provide a broad spectrum for evaluating the influence of PCM domain geometry under both low-temperature and high-temperature thermal energy storage conditions.

Table 7. Characteristics of the Phase Change Materials Used in This Study

PCM	**Type**	**Melting Temperature (°C)**	**Latent Heat (kJ/kg)**	**Application**
RT42	Organic	38–43	165	Low-temperature TES
Coral Cornet 159A	Organic	52–62	200	Medium-temperature TES
Erythritol	Organic	118	339.8	High-temperature TES

Solar Salt	Inorganic	220	110–170	CSP & High-temperature TES

3.2 PCM Storage Tank Geometries

To investigate the influence of PCM domain geometry on thermal energy storage performance, several storage tank configurations were designed and manufactured. The geometries were developed while maintaining an approximately constant PCM volume to ensure a fair comparison between different configurations.

The primary objective of the geometric modifications was to evaluate the effects of heat transfer surface distribution, PCM domain shape, and heat transfer distance on melting behavior and charging performance. Different tube arrangements were considered to analyze how geometry influences heat transfer mechanisms and melting front development within the PCM domain.

The designed geometries were manufactured using plexiglass to allow direct observation of the melting process and the evolution of the melting front during experiments. All configurations were integrated into the same experimental setup and tested under identical operating conditions.

3.2.1 Centered Single-Tube Geometry

The centered single-tube geometry was developed as the baseline configuration for experimental investigation. The storage tank was designed with internal dimensions of 112 mm × 67 mm × 150 mm and manufactured from transparent plexiglass. A single copper tube with an outer diameter of 28 mm was positioned at the geometric center of the PCM domain.

The centered tube arrangement provides a symmetric heat transfer distribution around the heat transfer surface. During the charging process, heat is transferred from the circulating heat transfer fluid to the surrounding PCM, initiating the melting process around the tube surface. As melting progresses, natural convection develops within the liquid PCM region and influences the melting front evolution.

This geometry was selected as the reference configuration for evaluating the effects of tube position and heat transfer surface arrangement on thermal performance.

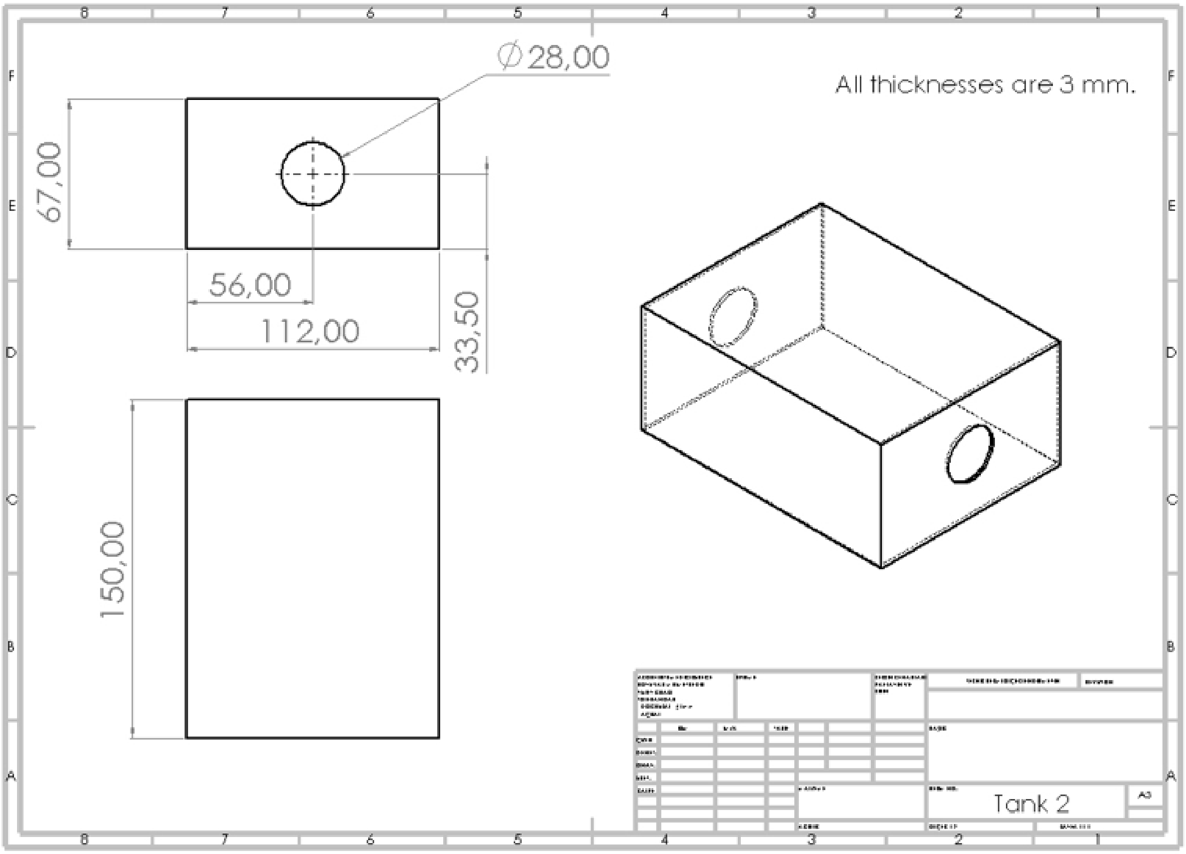

Figure 2. Technical Drawing of Single Tube Centered Configuration

3.2.2 Eccentric Single-Tube Geometry

The eccentric single-tube geometry was developed by relocating the heat transfer tube closer to the bottom wall of the storage tank while maintaining the same tank dimensions, tube diameter, and PCM volume as the centered single-tube configuration.

In this configuration, the tube center was positioned 19 mm above the bottom wall of the tank. Since the copper tube has an outer diameter of 28 mm, this arrangement provides a 5 mm clearance between the lower surface of the tube and the bottom wall. Compared with the centered single-tube geometry, this placement increases the available PCM volume above the heat transfer surface and provides a larger vertical region for buoyancy-driven flow during melting.

This geometry was selected to investigate the influence of tube position on melting behavior, natural convection development, and charging performance while keeping the heat transfer surface area constant.

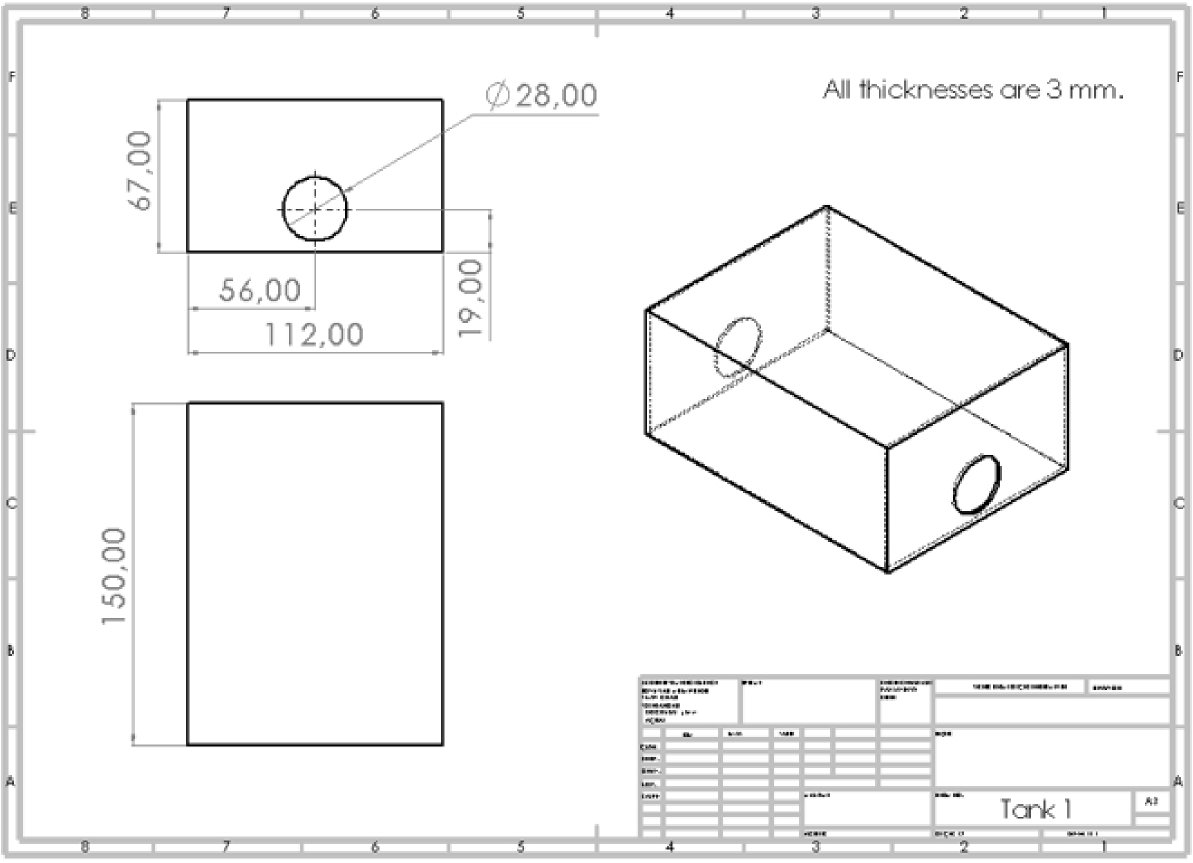

Figure 3. Technical Drawing of Single tube Eccentric Configuration

3.2.3 Centered Double-Tube Geometry

The centered double-tube geometry was developed to investigate the effect of increasing the heat transfer surface area within the PCM domain. Compared to the single-tube configurations, the number of heat transfer tubes was increased from one to two while maintaining an approximately constant PCM volume.

The storage tank was designed with internal dimensions of 122 mm × 67 mm × 150 mm and equipped with two copper tubes having an outer diameter of 28 mm. The tubes were positioned symmetrically within the PCM domain, with a center-to-center spacing of 40 mm. The spacing was determined by dividing the tank width into three approximately equal sections and locating the tube centers accordingly.

This arrangement provides a more uniform distribution of heat transfer surfaces throughout the PCM domain and reduces the average heat transfer distance between the PCM and the heated tubes. In addition, the selected spacing allows the melted regions around each tube to develop independently during the early stages of melting before interacting with each other.

This geometry was selected to evaluate the influence of increasing the number of heat transfer tubes on melting behavior, charging performance, and temperature distribution within the PCM domain.

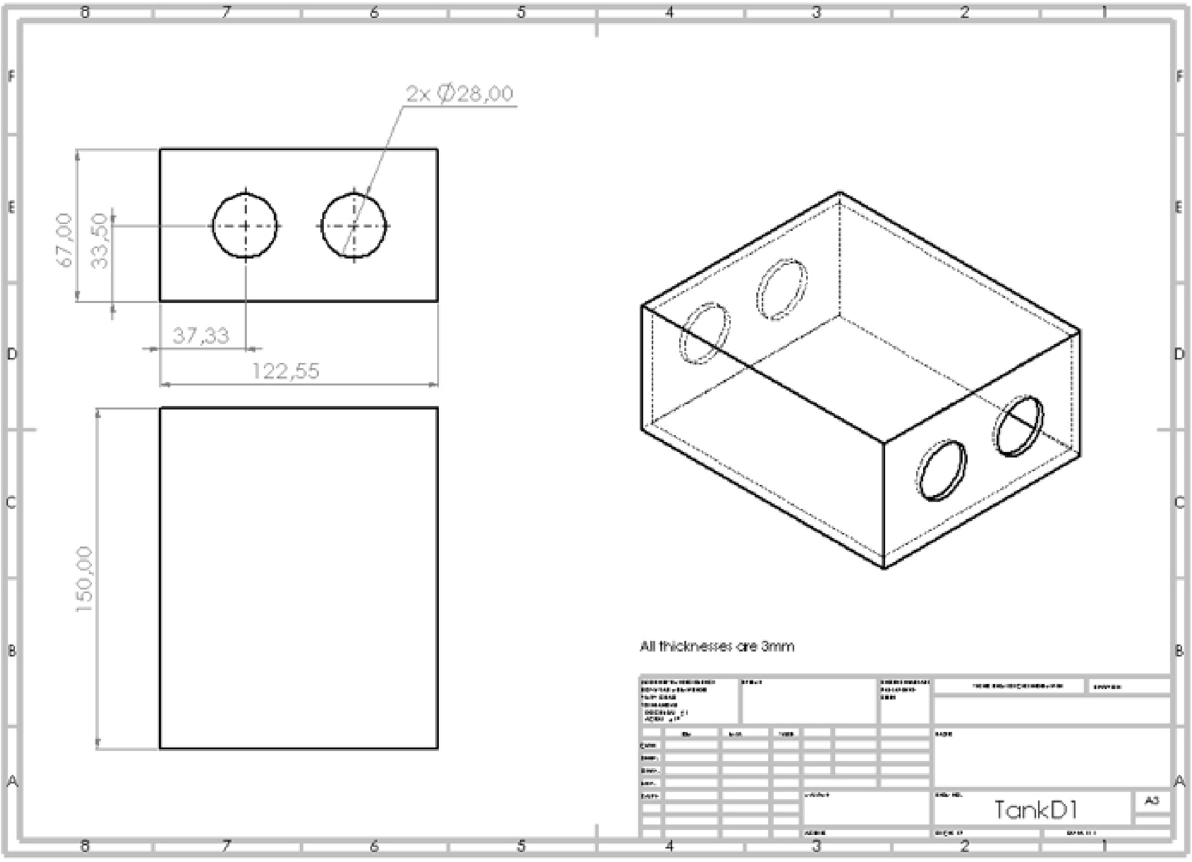

Figure 4. Technical Drawing of Double Tube Centered Configuration

3.2.4 Eccentric Double-Tube Geometry

The eccentric double-tube geometry was developed by relocating the two heat transfer tubes closer to the bottom wall of the storage tank while maintaining the same tank dimensions, tube diameter, and tube spacing as the centered double-tube configuration.

The design was inspired by the findings of Demirkıran and Çetkin [3], who demonstrated that eccentric tube arrangements can significantly enhance natural convection and reduce melting time in latent heat thermal energy storage systems. In the present configuration, both tube centers were positioned 19 mm above the bottom wall of the tank, creating a larger PCM region above the heat transfer surfaces.

By locating the tubes near the bottom of the PCM domain, buoyancy-driven flow is expected to develop more effectively during the melting process. The larger molten PCM region above the tubes allows natural convection currents to circulate more freely, accelerating heat transfer to the upper regions of the storage domain. Furthermore, the selected arrangement promotes a more efficient utilization of the PCM volume by reducing thermally inactive regions.

A clearance of 5 mm was maintained to ensure reliable manufacturing, sealing, and structural integrity of the storage tank. This geometry was selected to evaluate the combined effects of increased heat transfer surface area and eccentric tube positioning on the thermal performance of the PCM storage system.

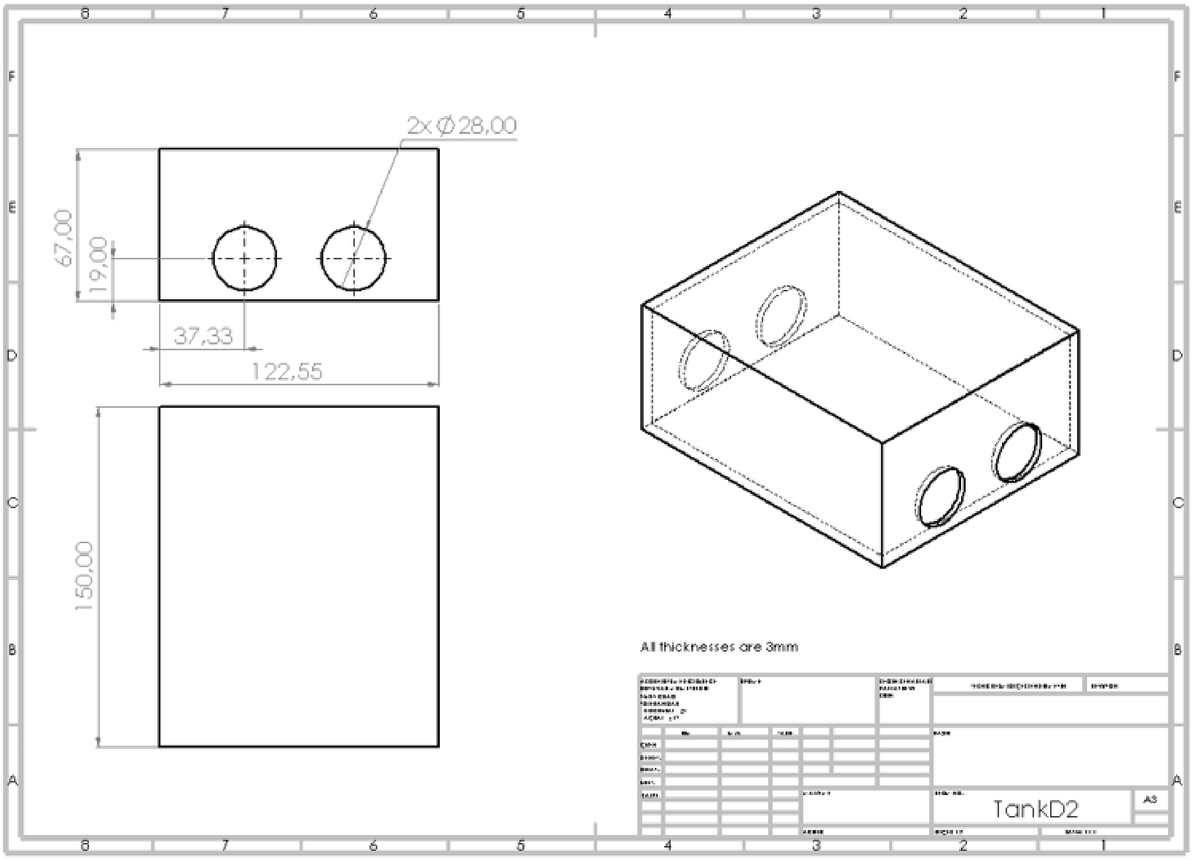

Figure 5. Technical Drawing of Double Tube Eccentric Tube Configuration

3.2.5 Finned Geometry

The finned geometry was developed to enhance heat transfer within the PCM domain while preserving the natural convection patterns that occur during melting. Previous studies have shown that increasing the heat transfer area through fins can significantly improve melting performance; however, excessive fin usage may suppress natural convection and reduce the overall effectiveness of latent heat storage systems [4].

The design consists of a single copper tube equipped with three longitudinal fins extending throughout the tank depth of 150 mm. Two fins were positioned symmetrically on the sides of the tube, while a third fin was placed vertically below the tube. All fins were manufactured from copper with a thickness of 1 mm.

The selected fin arrangement was intended to transfer heat more effectively toward the lower and lateral regions of the PCM domain, where melting is generally slower due to the limited influence of natural convection. At the same time, large open regions were intentionally preserved above the tube to allow buoyancy-driven flow to develop during the melting process.

Unlike dense fin configurations that may restrict fluid circulation within the molten PCM, the proposed three-fin geometry aims to establish a balance between conductive heat transfer enhancement and natural convection effects. Therefore, the finned configuration was included in the study to evaluate whether additional heat transfer surfaces could improve charging performance without significantly hindering the melting mechanisms observed in the non-finned geometries.

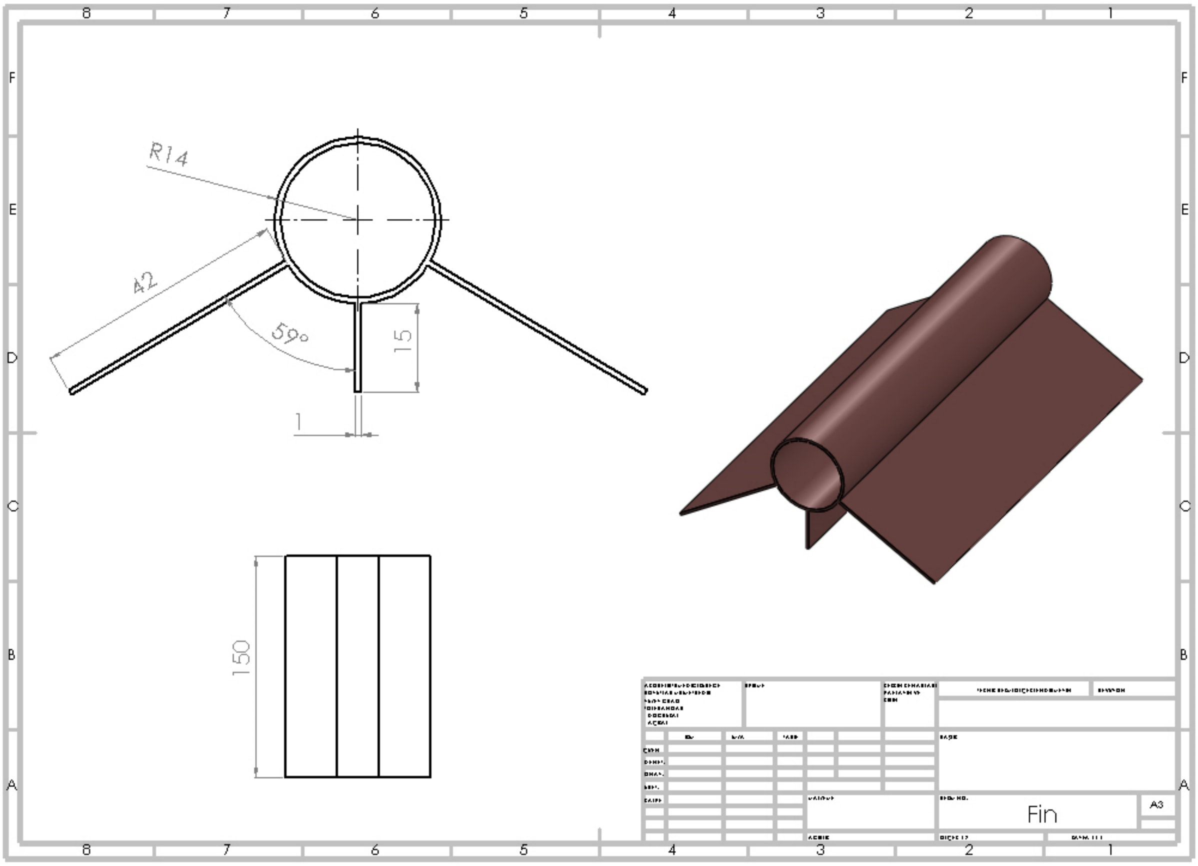

Figure 6. Technical Drawing of the Fins

Table 8. Specifications of the PCM Storage Tank Geometries

Geometry	Tube Number	Position	PCM Volume (L)
G1	1	Centered	1.03
G2	1	Eccentric	1.03
G3	2	Centered	1.04
G4	2	Eccentric	1.04
G5	1 + 3 Fins	Centered	1.03

3.3 Design Rationale

The geometries investigated in this study were selected to evaluate the influence of tube position, heat transfer surface area, and conduction enhancement techniques on the thermal performance of latent heat thermal energy storage systems. All configurations were designed with approximately the same PCM volume to ensure a fair comparison between different geometric arrangements.

The comparison between the centered and eccentric tube configurations was intended to investigate the effect of natural convection on the melting process. Previous studies have shown that locating heat transfer tubes near the bottom region of the storage domain can enhance buoyancy-driven flow and improve melting performance [3].

The comparison between single-tube and double-tube configurations was performed to evaluate the influence of heat transfer surface area. Increasing the number of tubes increases the contact area between the heat transfer fluid and PCM while reducing the average heat transfer distance within the storage domain.

Finally, the finned geometry was included to investigate the effect of conduction enhancement. Due to the inherently low thermal conductivity of most PCMs, fins are commonly employed to improve heat transfer and accelerate melting. The selected fin arrangement was designed to increase the effective heat transfer area while preserving sufficient space for natural convection to develop within the molten PCM [4].

Through these geometric variations, the study aims to identify the most effective PCM domain configuration for thermal energy storage applications and future solar thermal integration.

3.4 Material Selection

The material selection process was performed based on the thermal performance, manufacturability, cost, availability and compatibility with the experimental setup. The storage tank, heat transfer tubes, fins and phase change materials were chosen individually.

3.4.1 Storage Tank Material

Plexiglass (PMMA) was selected as the PCM storage tank material due to its transparency, low cost, and ease of fabrication. The transparent structure of plexiglass enabled direct observation of the melting front evolution during the experiments, which was one of the primary objectives of this study. In addition, plexiglass sheets can be easily machined and assembled, making them suitable for rapid prototyping and laboratory-scale testing.

The storage tanks were manufactured using 3 mm thick plexiglass sheets. The joints were sealed using acrylic adhesive and high-temperature silicone to ensure leak-free operation during charging and discharging experiments.

3.4.2 Heat Transfer Tube & Fin Material

Copper was selected as the heat transfer tube material because of its high thermal conductivity and widespread use in thermal energy storage applications. The high thermal conductivity of copper allows efficient heat transfer from the heat transfer fluid to the surrounding PCM, reducing thermal resistance during the charging process.

All geometries utilized copper tubes with an outer diameter of 28 mm. The tubes served as the primary heat transfer surfaces between the heat transfer fluid and the PCM domain.

Copper was also selected for the fins used in the finned geometry. Using the same material for both the tube and fins minimizes thermal contact resistance and ensures efficient heat transfer throughout the fin structure. The fins were designed to increase the effective heat transfer area and improve heat conduction to regions of the PCM that are located farther from the heat transfer tube.

3.4.3 Phase Change Materials

Four different phase change materials were selected to investigate the influence of PCM properties and operating temperature range on thermal energy storage performance. The thermophysical properties of the selected PCMs were presented previously in Section 3.1.

3.5 Experimental Setup

To evaluate the thermal performance of the proposed PCM storage geometries, two experimental systems were developed. The first system was designed for low-temperature PCMs using a water-based heat transfer loop, while the second system was developed for high-temperature PCMs and solar thermal integration using a parabolic dish collector and thermal oil circuit. Both systems were designed and assembled as part of the project.

3.5.1 System Components

The main components used in the experimental setups are summarized in Table 9.

Table 9. Specifications of the components used in the system

Component	Specification
Storage Tank Material	Plexiglass (PMMA), 3 mm thickness
Heat Transfer Tube	Copper, Ø28 mm outer diameter
Fin Material	Copper, 1 mm thickness
Temperature Sensor	K-type thermocouple
Number of Thermocouples	20
Heat Transfer Fluid (Low Temperature)	Water
Flow Rate (Low Temperature)	2.14 L/min
Flow Control Element	Ball valve
Heating Unit	Temperature-controlled circulator
Heat Transfer Fluid (High Temperature)	Dielectric thermal oil
Oil Circulation Unit	MAIS automotive oil pump
Pump Drive System	24 V DC motor
Solar Collector	Parabolic dish collector

Additional details regarding the operation and integration of these components are presented in the following sections.

3.5.2 Low-Temperature Experimental Setup

The low-temperature experimental setup was developed to investigate the melting behavior of RT42 and Coral Cornet 159A under controlled laboratory conditions. The system consisted of a temperature-controlled circulator, control valves, connecting pipes, and a PCM storage tank.

The circulator supplied hot water at a constant temperature and flow rate through the copper tube embedded within the PCM domain. Throughout the experiments, the water flow rate was maintained at approximately 2.14 L/min. The copper tube was assumed to operate under a constant wall temperature condition due to the high circulation rate and stable inlet temperature provided by the circulator.

To monitor the thermal behavior of the system, twenty K-type thermocouples were installed at different locations. Thermocouples were positioned inside the PCM domain, on the tube outlet, tank outlet surfaces, and on the room temperature. Temperature measurements were continuously recorded throughout the charging process to analyze melting characteristics and thermal response.

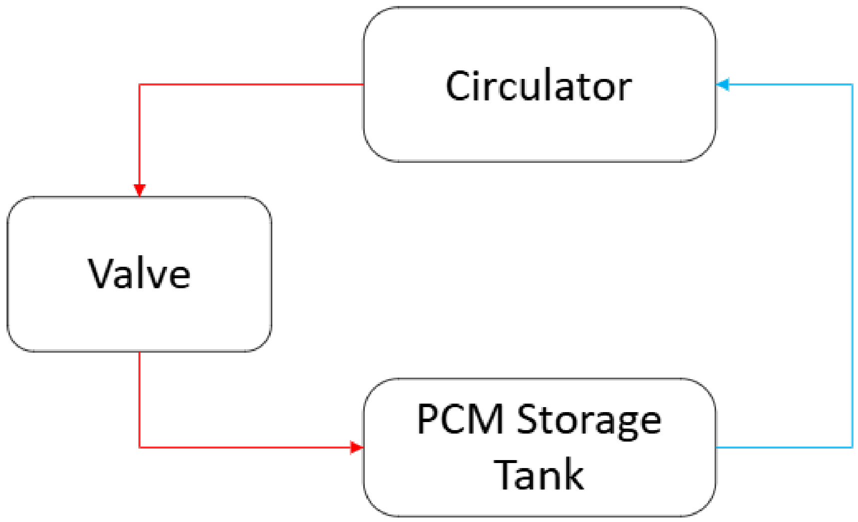

Figure 7. Low Temperature Experimental Setup

The transparent plexiglass tank enabled direct observation of the melting front evolution, allowing visual comparison of the different geometric configurations.

3.5.3 High-Temperature Solar Experimental Setup

The second experimental setup was developed to investigate the applicability of the selected PCM geometries under high-temperature operating conditions and to evaluate their potential for solar thermal energy storage applications.

The system consists of a parabolic dish solar collector, a thermal oil storage tank, an oil circulation pump, a DC motor drive system, piping, and the PCM storage unit. Unlike the low-temperature setup, thermal oil was selected as the heat transfer fluid due to the elevated operating temperatures required for Erythritol and Solar Salt.

Solar radiation is concentrated at the focal region of the parabolic dish collector, where the thermal oil tank is positioned. The heated oil is circulated through the PCM storage unit, transferring thermal energy to the PCM during the charging process. The circulation system is driven by a DC motor coupled to the pump mechanism.

Temperature measurements are obtained using thermocouples located within the PCM domain, on the heat transfer tube surfaces, and at critical points of the thermal oil circuit. These measurements are used to evaluate charging performance, temperature distribution, and melting characteristics under solar heating conditions.

The high-temperature setup was designed as the second phase of the project to investigate the feasibility of integrating latent heat thermal energy storage with concentrated solar thermal systems.

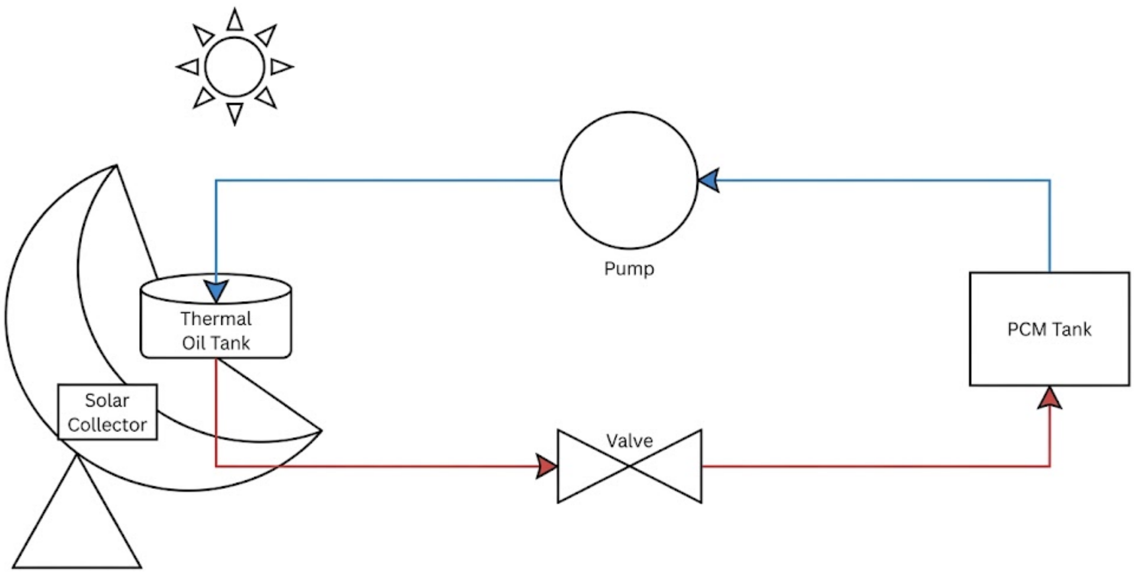

Figure 8. High-temperature solar thermal experimental setup.

3.5.4 Instrumentation and Temperature Measurement

Approximately twenty K-type thermocouples were used to monitor the temperature variation during the experiments. The thermocouples were distributed throughout the experimental setup to capture the thermal response of the PCM storage system and evaluate the heat transfer characteristics during the charging process.

The main measurement locations were selected as the PCM domain, water outlet, external tank surface, and ambient environment. Thermocouples placed inside the PCM domain were used to evaluate temperature distribution and melting behavior. The water outlet thermocouple was used to monitor the heat transfer fluid temperature after passing through the PCM tank. Additional thermocouples on the outer tank surface and in the ambient environment were used to observe heat losses and surrounding temperature conditions.

The collected temperature data were used to compare the charging performance of different geometries and to support the analysis of melting front development.

3.6 Engineering Calculations

Engineering calculations were performed to evaluate the thermal and fluid flow characteristics of the proposed latent heat thermal energy storage systems. These calculations provide a theoretical basis for comparing different PCM domain geometries and assessing their charging performance. The selected parameters were chosen based on the governing heat transfer mechanisms within the storage unit, including conduction, forced convection, and natural convection. In addition, energy storage capacity and heat transfer characteristics were evaluated using the thermophysical properties of the selected phase change materials and heat transfer fluids.

3.6.1 Assumptions

The following assumptions were adopted for the engineering calculations and analysis of the PCM storage systems:

- The PCM was initially at a uniform temperature throughout the storage tank.
- The thermophysical properties of each PCM were assumed to be constant within the solid and liquid phases.
- The HTF properties were assumed to be constant during the charging process.
- Due to the short tube length and controlled operating conditions, the temperature drop of the HTF along the tube was assumed to be negligible.
- Therefore, the copper tube wall temperature was considered approximately constant during charging.
- The copper tube was assumed to be homogeneous and isotropic, and its thermal resistance was considered negligible compared to the thermal resistance of the PCM.
- Heat losses to the surroundings were neglected in theoretical calculations.
- The PCM volume was assumed to remain constant during phase change.
- Natural convection effects within the molten PCM were represented through Rayleigh number analysis.

3.6.2 PCM Volume Calculation

The net PCM volume was calculated by subtracting the volume occupied by the copper tube or tubes from the internal tank volume. This calculation was performed to verify that all geometries contain approximately the same PCM volume, allowing a fair comparison between different tank configurations.

For the single-tube geometries, the internal tank dimensions are 112 mm × 67 mm × 150 mm, and the tube outer diameter is 28 mm. The resulting net PCM volume is approximately 1.033 L**.**

For the double-tube geometries, the internal tank dimensions are 122 mm × 67 mm × 150 mm. Since two copper tubes are used, the total tube volume is subtracted from the tank volume. The resulting net PCM volume is approximately 1.041 L**.**

Table 10. Dimensions and Tube Configurations of the Investigated PCM Storage Tanks

Geometry	Tank Dimensions (mm)	Tube Configuration	Net PCM Volume (L)
G1	112 × 67 × 150	Centered single tube	1.033
G2	112 × 67 × 150	Eccentric single tube	1.033
G3	122 × 67 × 150	Centered double tube	1.041
G4	122 × 67 × 150	Eccentric double tube	1.041
G5	112 × 67 × 150	Finned single tube	~1.03

The calculated volumes show that the PCM amount was kept nearly constant for all main geometries. Therefore, the observed performance differences can be mainly attributed to geometric parameters such as tube position, number of tubes, and heat transfer surface area. Furthermore, a PCM volume of approximately 1 L was selected as a compromise between experimental feasibility and representative thermal storage capacity. This volume provides a sufficiently large PCM domain to observe melting front evolution and natural convection effects while remaining practical for laboratory-scale manufacturing, instrumentation, and testing.

3.6.3 Heat Transfer Surface Area Calculation

The heat transfer surface area is one of the most important parameters affecting the charging performance of latent heat thermal energy storage systems. Increasing the available heat transfer area enhances the thermal interaction between the HTF and the PCM, resulting in faster heat transfer and accelerated melting.

In the present study, heat transfer occurs through the external surfaces of the copper tubes and fins. Therefore, the outer surface area was considered as the effective heat transfer area. The heat transfer area of a cylindrical tube was calculated using:

$$A = \pi D L$$

where D is the outer diameter of the tube and L is the tube length.

All investigated geometries utilize copper tubes with an outer diameter of 28 mm and a length of 150 mm. The calculated heat transfer area of a single tube is 0.0132 m^2. Since the centered and eccentric single-tube configurations employ identical tube dimensions, both geometries provide the same heat transfer area. Similarly, the centered and eccentric double-tube configurations have twice the heat transfer area of the single-tube designs, resulting in a total heat transfer area of 0.0264 m^2.

For the finned geometry, three longitudinal copper fins were attached to the tube. Two inclined fins and one bottom fin extend throughout the entire tank depth, increasing the available heat transfer surface between the heat source and the PCM. Including the contribution of the fins, the total heat transfer area of the finned configuration was calculated as 0.0435 m^2.

The calculated heat transfer areas for all geometries investigated are summarized in Table 11. The results show that the finned geometry provides the largest heat transfer area, followed by the double-tube and single-tube configurations. Therefore, variations in melting performance are expected to be influenced not only by natural convection effects but also by differences in the available heat transfer surface area.

Table 11. Heat Transfer Surface Areas of the Investigated Geometries

Geometry	**Configuration**	**Heat Transfer Area (m^2)**
G1	Centered Single-Tube	0.0132
G2	Eccentric Single-Tube	0.0132
G3	Centered Double-Tube	0.0264
G4	Eccentric Double-Tube	0.0264
G5	Finned Geometry	0.0435

3.6.4 Flow Characterization

The flow characteristics of the heat transfer fluid were evaluated using the Reynolds and Prandtl numbers. These dimensionless parameters were used to characterize the flow regime and thermal behavior inside the copper tube and were subsequently utilized in the convective heat transfer calculations.

3.6.4.1 Reynolds Number

The flow characteristics of the heat transfer fluid were evaluated using the Reynolds number. The Reynolds number was calculated to determine the flow regime inside the copper tube during the charging process.

$$Re = \frac{\rho V D}{\mu}$$

where $\rho$is the density of water, $V$is the average flow velocity, $D$is the tube diameter, and $\mu$is the dynamic viscosity of water.

For the calculations, the inlet water temperature was taken as 65°C and the volumetric flow rate was 2.14 L/min. The same flow rate was used for both single-tube and double-tube geometries since, in the double-tube configuration, the flow passes from one tube to the other without splitting.

The volumetric flow rate was converted as:

$$Q = 2.14 \text{ L/min} = 3.57 \times 10^{-5} \text{ m}^3/\text{s}$$

The average flow velocity inside the tube was calculated as:

$$V = \frac{Q}{A}$$

Using a tube diameter of 28 mm:

$$V = 0.058 \text{ m/s}$$

At 65°C, the properties of water were taken approximately as:

$$\rho = 980 \text{ kg/m}^3$$
$$\mu = 4.35 \times 10^{-4} \text{ Pa.s}$$

Therefore, the Reynolds number was calculated as:

$$Re = \frac{(980)(0.058)(0.028)}{4.35 \times 10^{-4}}$$
$$Re \approx 3650$$

Since the Reynolds number is higher than 2300, the flow is in the transitional region. Therefore, forced convection inside the copper tube contributes significantly to heat transfer from the water to the PCM storage domain.

3.6.4.2 Prandtl Number

The Prandtl number was calculated to characterize the relative thickness of the momentum and thermal boundary layers of the heat transfer fluid. It is defined as:

$$Pr = \frac{\mu c_p}{k}$$

where $\mu$is the dynamic viscosity, $c_p$is the specific heat capacity, and $k$is the thermal conductivity of water.

For water at 65°C, the properties were taken as:

$$\mu = 4.35 \times 10^{-4} \text{ Pa.s}$$
$$c_p = 4180 \text{ J/kg.K}$$
$$k = 0.656 \text{ W/m.K}$$

Therefore:

$$Pr = \frac{(4.35 \times 10^{-4})(4180)}{0.656}$$
$$Pr \approx 2.77$$

The calculated Prandtl number shows that thermal diffusion and momentum diffusion are both significant for the water flow inside the copper tube. This value was later used in the Nusselt number calculation for forced convection analysis.

3.6.5 Convective Heat Transfer Analysis

Convective heat transfer between the heat transfer fluid and the copper tube was evaluated using the Nusselt number and convective heat transfer coefficient. These parameters were calculated based on the Reynolds and Prandtl numbers obtained previously.

3.6.5.1 Nusselt Number

The Nusselt number represents the ratio of convective heat transfer to conductive heat transfer within a fluid. It is commonly used to evaluate the effectiveness of heat transfer in internal flow systems.

Since the calculated Reynolds number falls within the transitional flow regime, the Gnielinski correlation was employed to estimate the Nusselt number:

$$Nu = \frac{(f/8)(Re - 1000)Pr}{1 + 12.7(f/8)^{1/2}(Pr^{2/3} - 1)}$$

where $f$is the Darcy friction factor, $Re$is the Reynolds number, and $Pr$is the Prandtl number.

The friction factor was calculated using:

$$f = (0.79 \ln\ Re - 1.64)^{-2}$$

Using the previously calculated values of $Re = 3650$and $Pr = 2.77$, the Nusselt number was determined as:

$$Nu \approx 18$$

The obtained Nusselt number indicates that convective heat transfer within the copper tube is significantly enhanced compared to pure conduction. This enhanced heat transfer contributes to the effective delivery of thermal energy from HTF to the PCM storage domain during the charging process.

3.6.5.2 Convective Heat Transfer Coefficient

The convective heat transfer coefficient was calculated using the Nusselt number obtained in the previous section. The relationship between the Nusselt number and the convective heat transfer coefficient is given by:

$$Nu = \frac{hD}{k}$$

Rearranging the equation for the convective heat transfer coefficient yields:

$$h = \frac{Nu\,k}{D}$$

where $Nu$is the Nusselt number, $k$is the thermal conductivity of water, and $D$is the tube diameter.

Using the previously calculated Nusselt number ($Nu = 18$), a thermal conductivity of water at 65°C of $k = 0.656$ W/m.K, and a tube diameter of $D = 0.028$ m, the convective heat transfer coefficient was calculated as:

$$h = \frac{(18)(0.656)}{0.028}$$

$$h \approx 422 \text{ W/m}^2\text{K}$$

The calculated value indicates effective convective heat transfer between the heat transfer fluid and the inner surface of the copper tube, supporting efficient thermal energy transfer to the PCM domain during charging.

3.6.6 Natural Convection Analysis

3.6.6.1 Characteristic Length

In this study, the Rayleigh number was used as a comparative parameter to evaluate the natural convection potential of different PCM domain geometries. Since natural convection during melting is mainly driven by buoyancy, the vertical PCM region above the heated tube was selected as the primary characteristic length.

For the centered tube geometry:

$$L_c = 67 - (33.5 + 14) = 19.5\ mm = 0.0195\ m$$

For the eccentric tube geometry:

$$L_c = 67 - (19 + 14) = 34\ mm = 0.034\ m$$

Horizontal characteristic lengths were also calculated to compare the side and middle PCM regions:

$$L_{c,h,single} = \frac{112 - 28}{2} = 42\ mm = 0.042\ m$$
$$L_{c,h,double,side} = 27\ mm = 0.027\ m$$
$$L_{c,h,double,middle} = 12\ mm = 0.012\ m$$

3.6.6.2 Rayleigh Number

The Rayleigh number was calculated using:

$$Ra = \frac{g\beta\Delta T L_c^3}{\nu\alpha}$$

For RT42 at 65°C water temperature:

$$\Delta T = 65 - 42 = 23K$$
$$\rho = 760\ kg/m^3, \mu = 0.003\ Pa \cdot s$$
$$k = 0.15\ W/mK, c_p = 2400\ J/kgK, \beta = 0.001\ K^{-1}$$
$$\nu = \frac{\mu}{\rho} = 3.95 \times 10^{-6}\ m^2/s$$
$$\alpha = \frac{k}{\rho c_p} = 8.22 \times 10^{-8}\ m^2/s$$

The calculated Rayleigh numbers are summarized in Table 12.

Table 12. Rayleigh Number Calculation for Different Geometrical Configurations

Case	Characteristic Length	L_c	Rayleigh Number
Centered tube vertical	PCM height above tube	19.5 mm	5.15×10^6
Eccentric tube vertical	PCM height above tube	34 mm	2.73×10^7
Single-tube horizontal	Side PCM distance	42 mm	5.15×10^7
Double-tube horizontal side	Wall-tube distance	27 mm	1.37×10^7
Double-tube middle region	Tube-to-tube PCM gap	12 mm	1.20×10^6

3.6.6.3 Effect of Tube Position on Natural Convection

The calculated Rayleigh numbers show that the eccentric tube position increases the vertical natural convection potential. By moving the tube closer to the bottom wall, the vertical PCM region above the tube increases from 19.5 mm to 34 mm. Since the Rayleigh number is proportional to L_c^3, this change increases the vertical Rayleigh number by approximately 5.3 times.

Therefore, the eccentric tube configurations are expected to support stronger buoyancy-driven flow and faster melting front development compared to the centered configurations. This calculation supports the design decision of placing the heat transfer tube near the bottom region of the PCM domain.

3.7 Experimental Results

This section presents the experimental results obtained from the charging and discharging tests conducted with RT42 PCM. The thermal behavior of the PCM domain was evaluated using temperature measurements recorded throughout both energy storage and energy release processes. Five different storage tank geometries were experimentally investigated to assess the influence of tube position, tube number, and fin implementation on thermal performance.

The experimental results are presented separately for each geometry to provide a clear comparison of their charging and discharging characteristics under identical operating conditions. The system performance was evaluated using temperature evolution within the PCM domain, inlet and outlet water temperatures, melting behavior during charging, and solidification behavior during discharging. All experiments were performed using the same PCM volume, tube diameter, flow rate, and operating conditions to ensure a consistent basis for comparison.

The following sections present the results obtained from the centered single-tube, eccentric single-tube, centered double-tube, eccentric double-tube, and finned geometries.

3.7.1 Centered Single-Tube Geometry

The centered single-tube geometry served as the reference configuration for the experimental study. In this design, the copper tube was positioned at the geometric center of the PCM domain, providing a symmetrical heat source within the PCM volume. Charging experiments were conducted using water at 65°C circulating through the copper tube at a constant flow rate of 2.14 L/min. Following the charging process, discharging experiments were performed to evaluate the thermal energy release characteristics of the storage unit.

Figure 9-10 presents the temperature evolution measured at different thermocouple locations during the charging and discharging processes. The recorded temperatures illustrate the heat transfer behavior within the PCM domain and provide insight into the melting and solidification characteristics of the storage system.

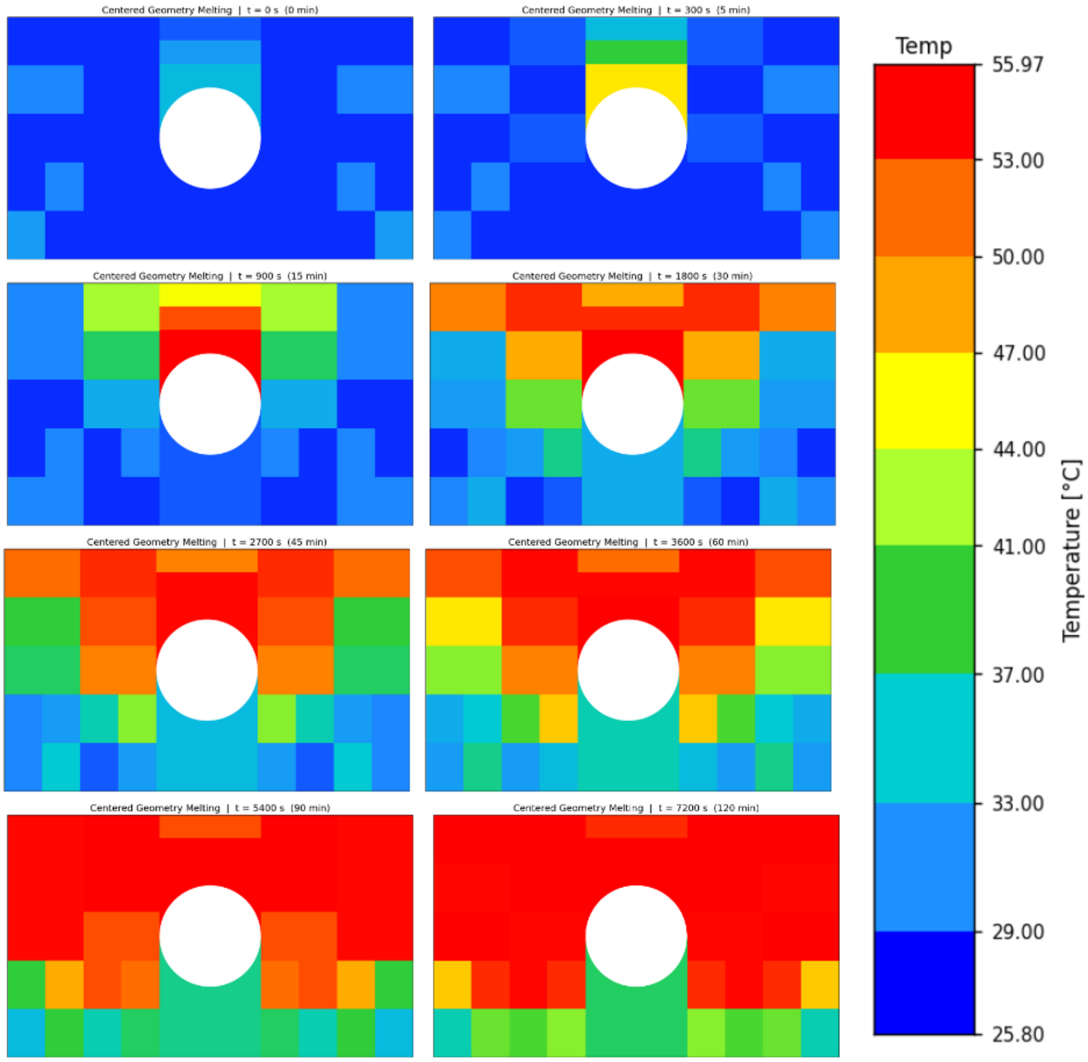

Figure 9. Melting of Centered Single Tube Geometry

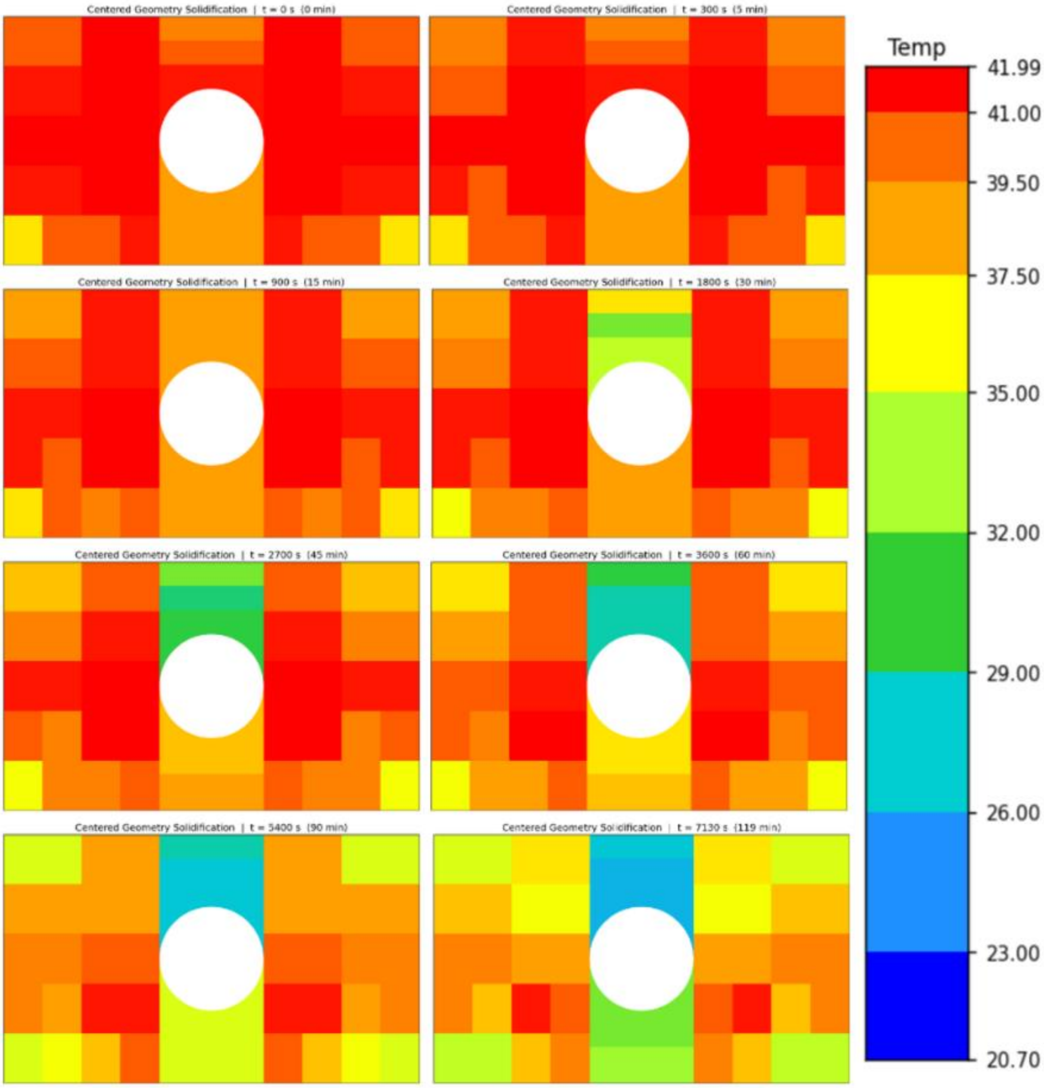

Figure 10. Solidifying of Centered Single Tube Geometry

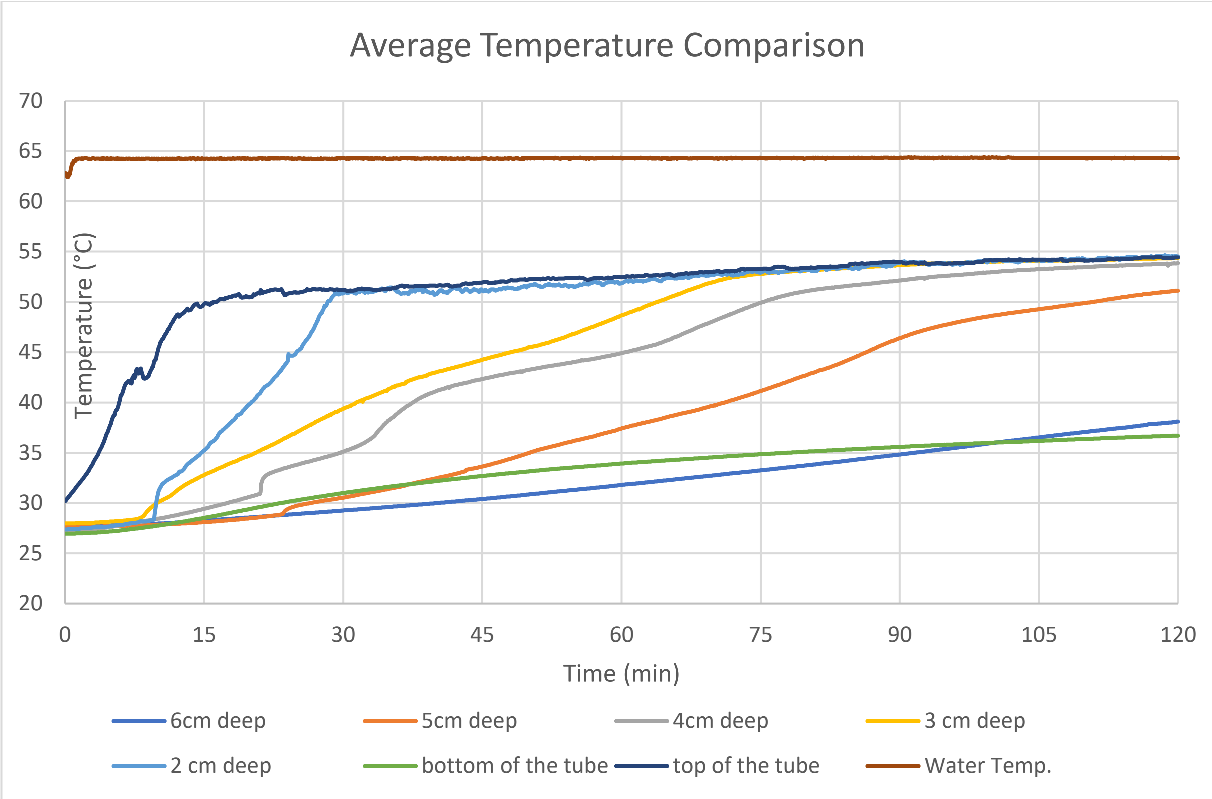

Figure 11. Average Temperature Distribution in centered geometry melting based on the depth of the thermocouple

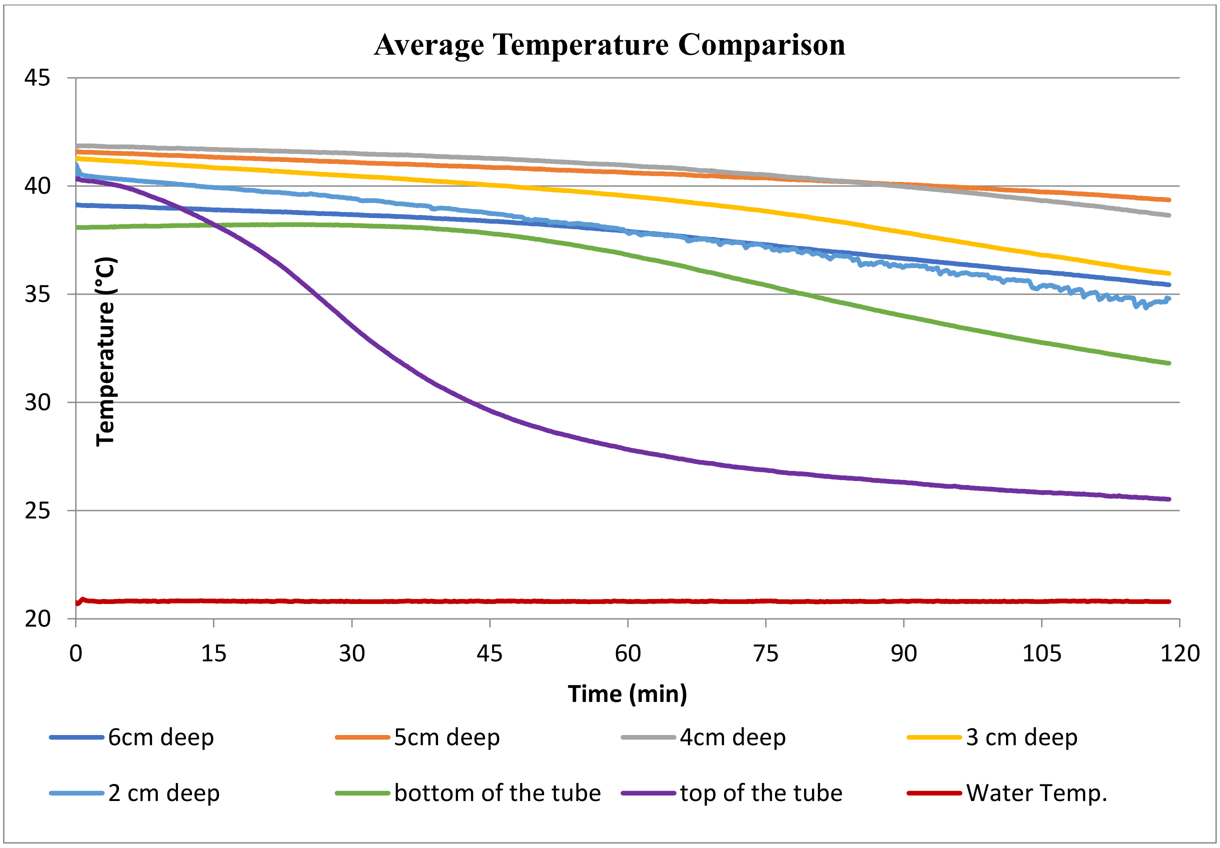

Figure 12. Average Temperature Distribution in centered geometry solidifying based on the depth of the thermocouple

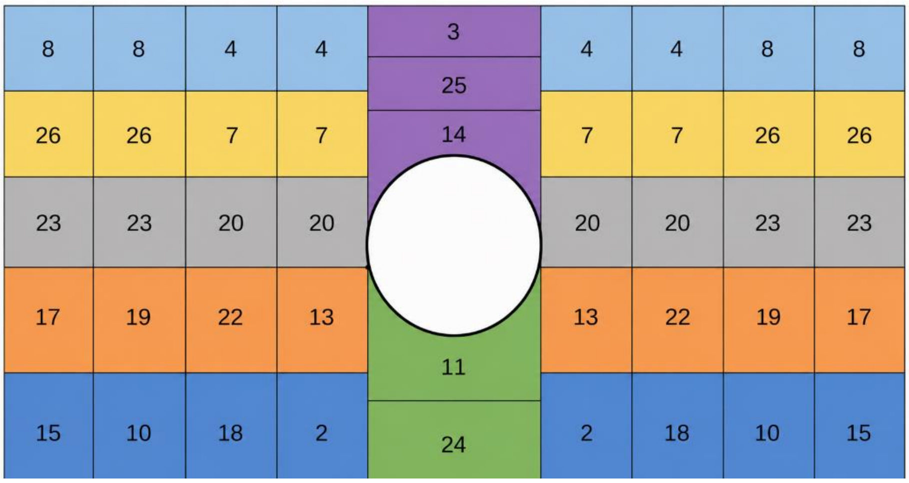

Figure 13. Thermocouple placement for centered geometry

The temperature distributions obtained during the charging process reveal that the upper region of the PCM domain experienced significantly faster heating than the lower region. While temperatures above the tube rapidly approached and exceeded the melting temperature of RT42, the bottom corners of the storage tank remained noticeably colder throughout the experiment.

This behavior can be attributed to buoyancy-driven natural convection within the molten PCM. As the PCM surrounding the heated tube melts, the warmer and less dense liquid rises toward the upper region of the tank, transporting thermal energy away from the heat source. Consequently, heat accumulates in the upper section of the storage domain, while the lower regions rely primarily on conduction, which is considerably slower than convective heat transfer.

As a result, melting was concentrated above the tube and a significant portion of the PCM located near the bottom corners remained at lower temperatures. This indicates that the centered single-tube geometry does not utilize the lower PCM volume effectively and leads to non-uniform thermal energy distribution within the storage tank. Similar temperature stratification was also observed during the discharging process, where the upper region retained thermal energy for a longer period than the lower section.

3.7.2 Eccentric Single-Tube Geometry

The eccentric single-tube geometry was designed to investigate the effect of tube position on the thermal performance of the PCM storage unit. In this configuration, the copper tube was positioned near the bottom wall of the storage tank, with a clearance of 5 mm between the tube and the lower surface. Similar to the centered configuration, charging experiments were conducted using water at 65°C circulating through the copper tube at a constant flow rate of 2.14 L/min. Following the charging process, discharging experiments were performed to evaluate the thermal energy release characteristics of the storage unit.

Figure 14-15 presents the temperature evolution measured at different thermocouple locations during the charging and discharging processes. The recorded temperatures illustrate the influence of the eccentric tube placement on heat transfer within the PCM domain and provide insight into the melting and solidification behavior of the storage system.

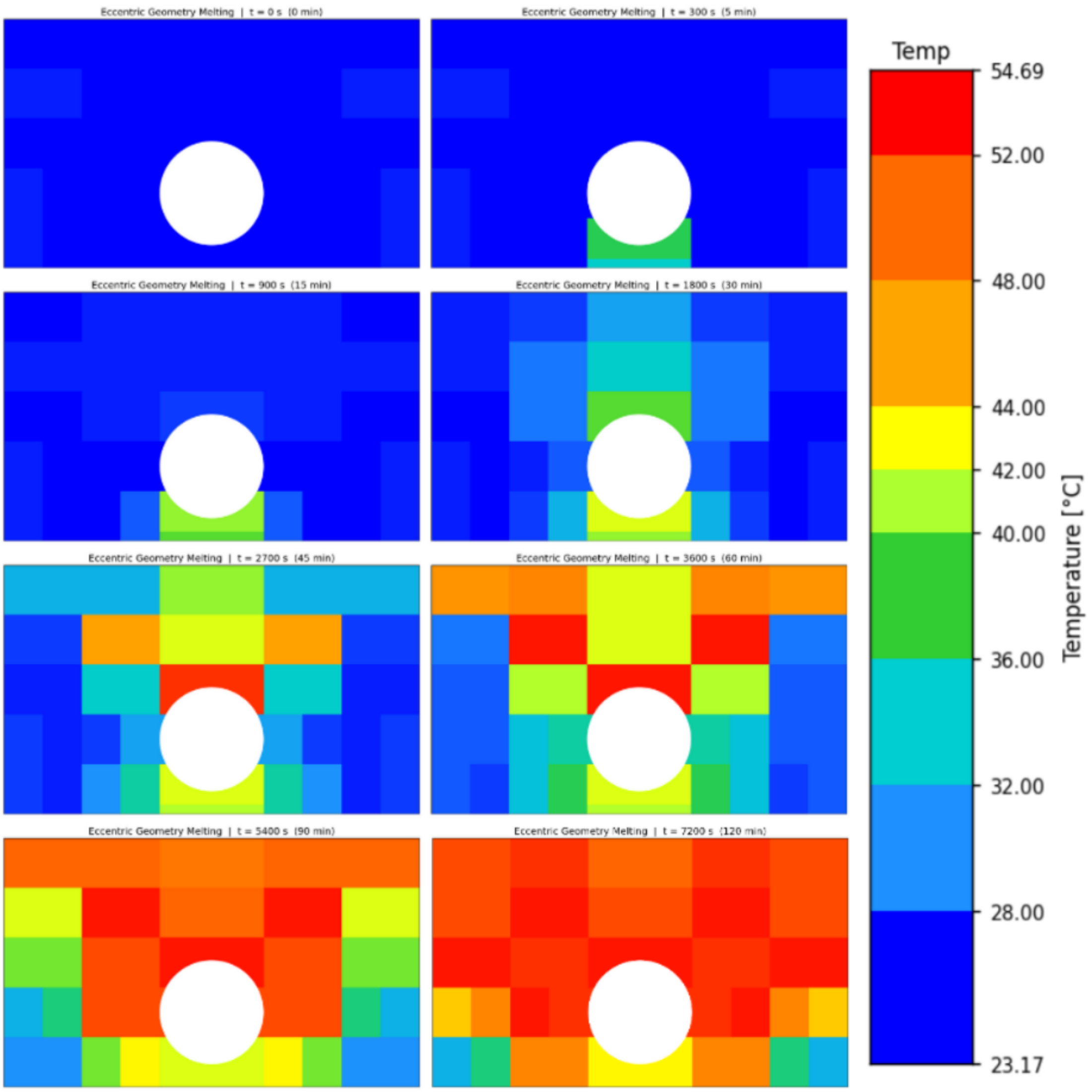

Figure 14. Melting of Eccentric Single Tube Geometry

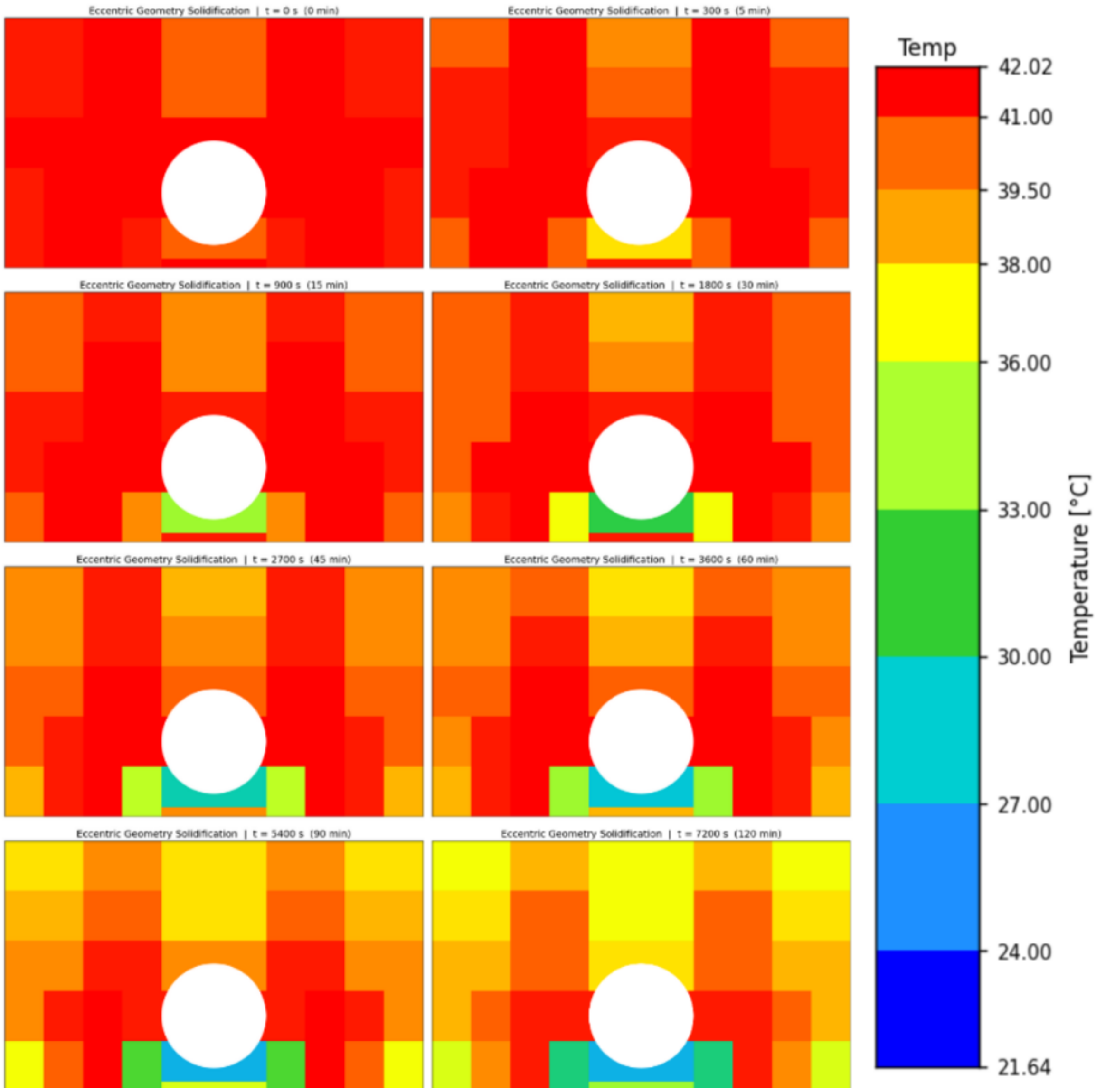

Figure 15. Solidifying of Eccentric Single Tube Geometry

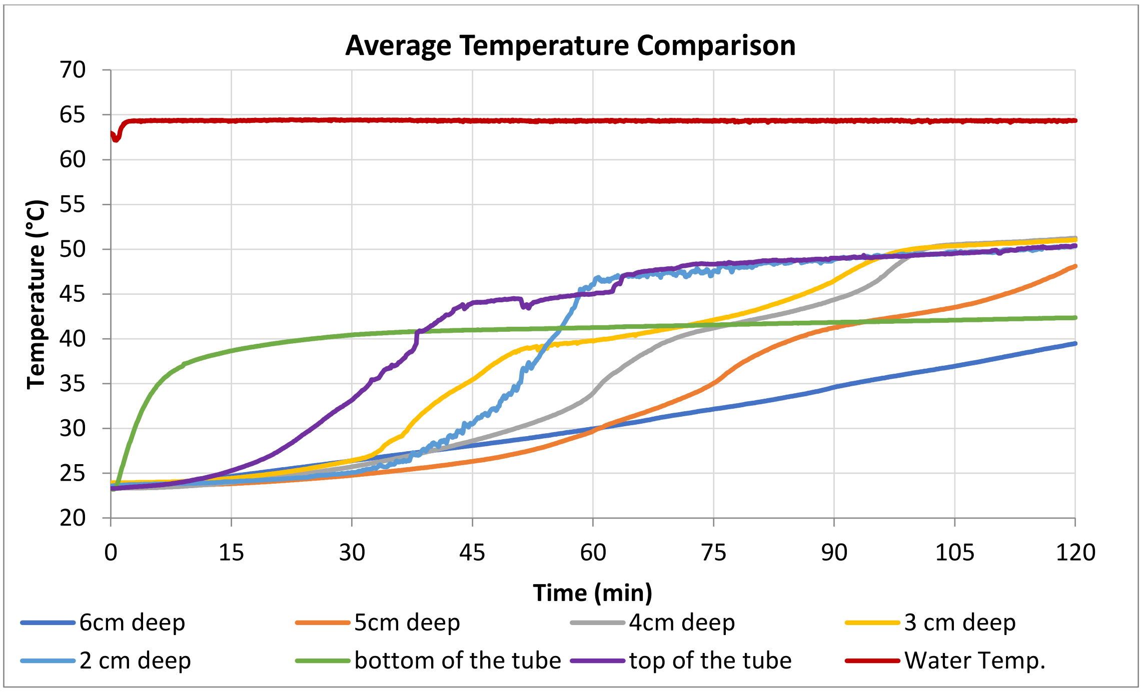

Figure 16. Average Temperature Distribution in eccentric geometry melting based on the depth of the thermocouple

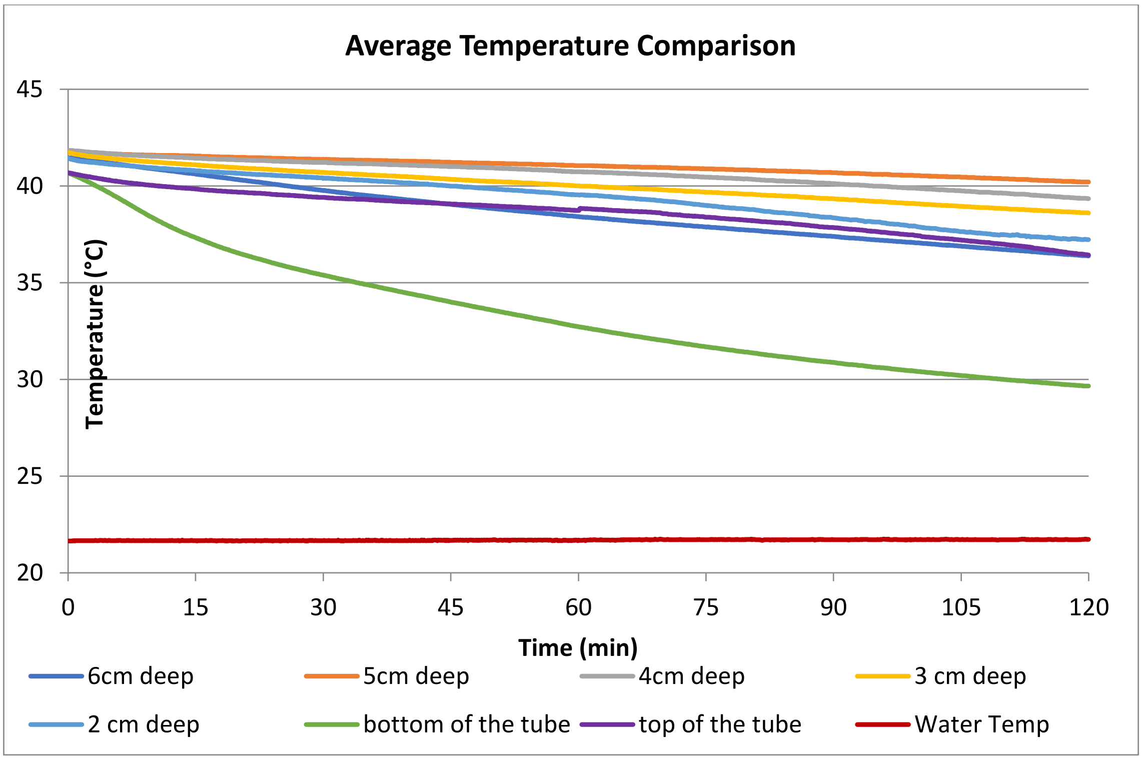

Figure 17.Average Temperature Distribution in eccentric geometry solidifying based on the depth of the thermocouple

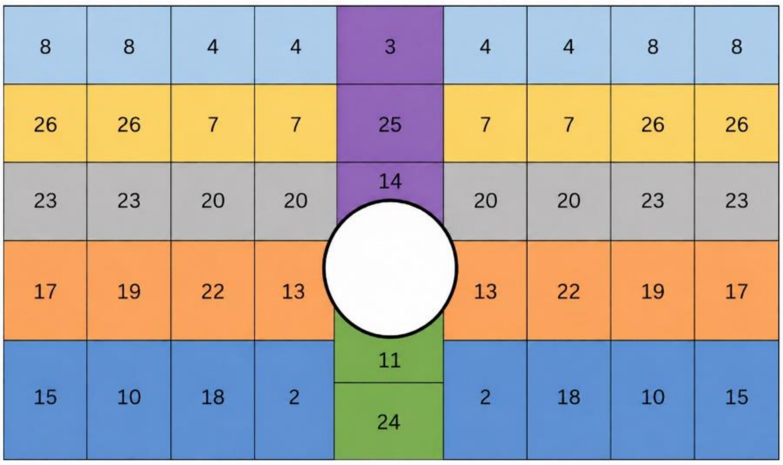

Figure 18. Thermocouple Placement for eccentric geometry

3.7.3 Centered Double-Tube Geometry

The centered double-tube geometry was developed to investigate the effect of increasing the heat transfer surface area within the PCM domain. In this configuration, two copper tubes were positioned symmetrically inside the storage tank, dividing the PCM volume into three approximately equal sections. This arrangement was intended to provide a more uniform heat distribution and reduce the maximum heat transfer distance between the heat source and the surrounding PCM.

Charging experiments were conducted using water at 65°C circulating through the tube network at a constant flow rate of 2.14 L/min. Following the charging process, discharging experiments were performed to evaluate the thermal energy release characteristics of the storage unit.

Figure 19-20 presents the temperature evolution measured at different thermocouple locations during the charging and discharging processes. The recorded temperatures illustrate the influence of the additional heat transfer tube on thermal distribution within the PCM domain and provide insight into the melting and solidification behavior of the storage system.

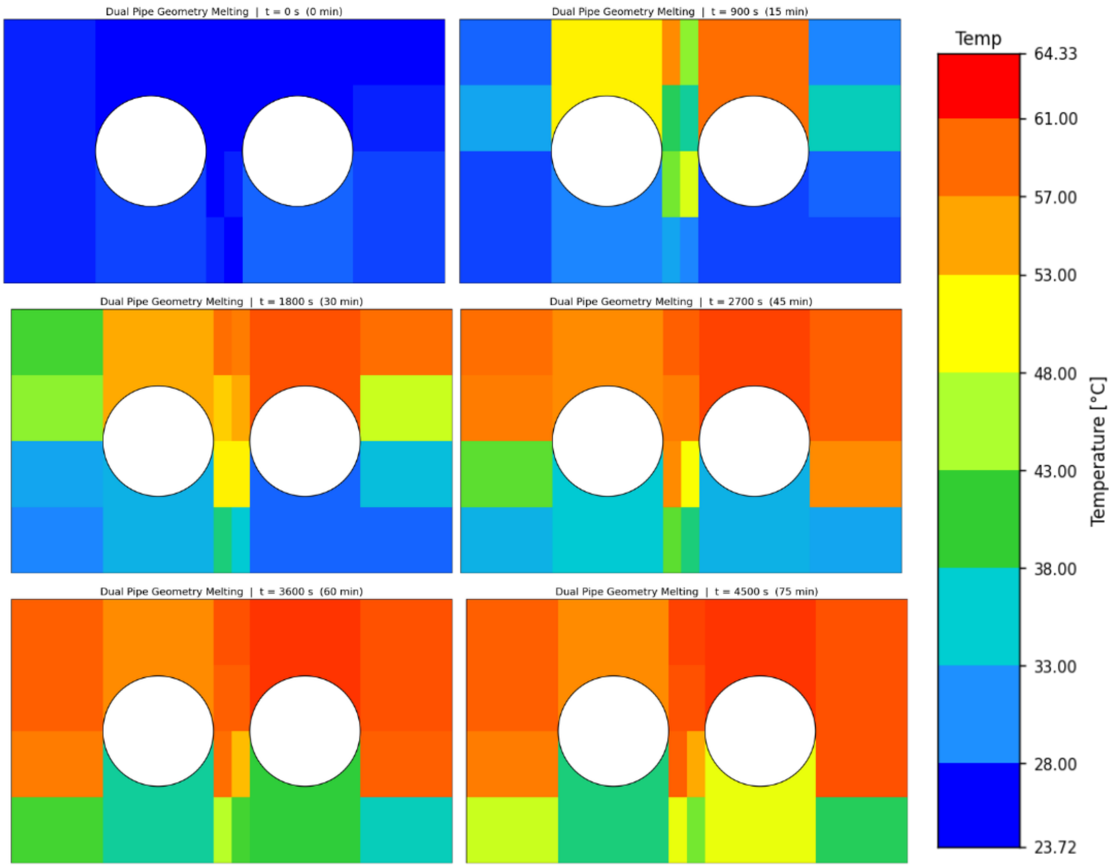

Figure 19. Melting of Double Tube Centered Geometry

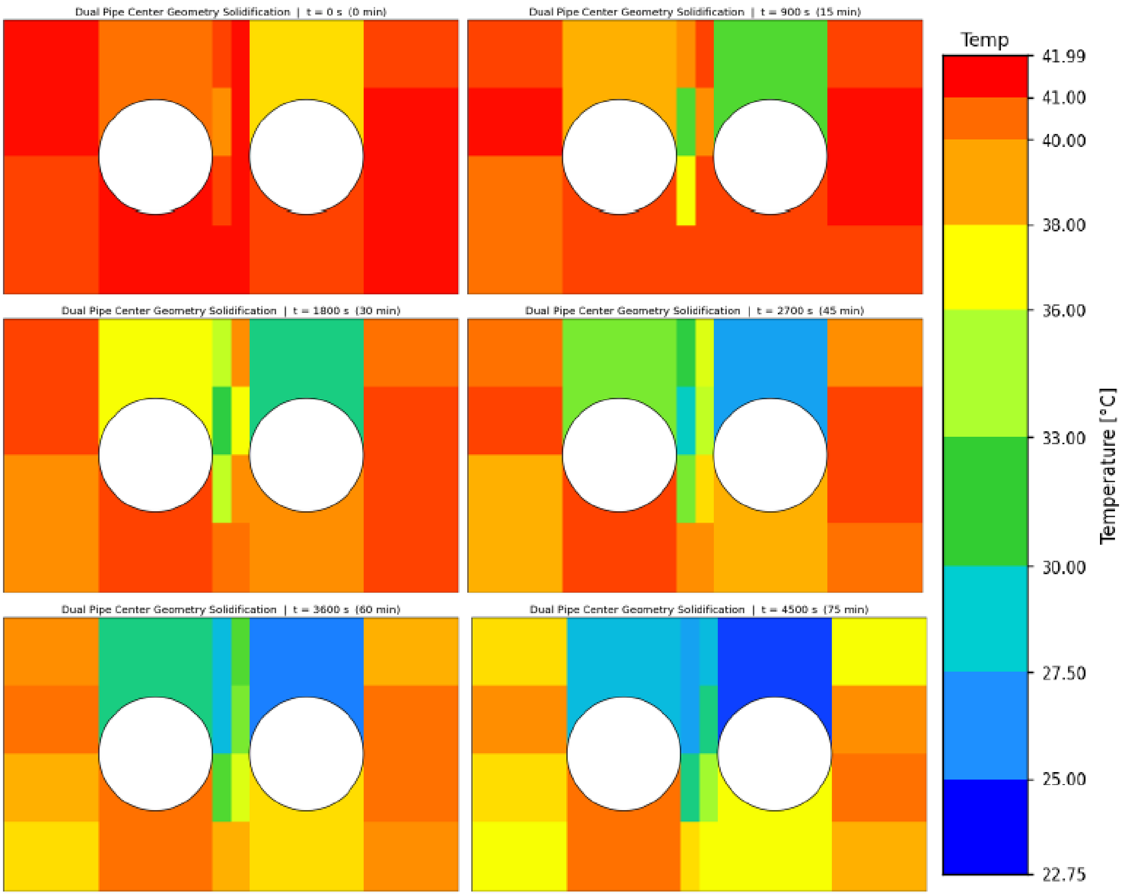

Figure 20. Solidifying of Double Tube Centered Geometry

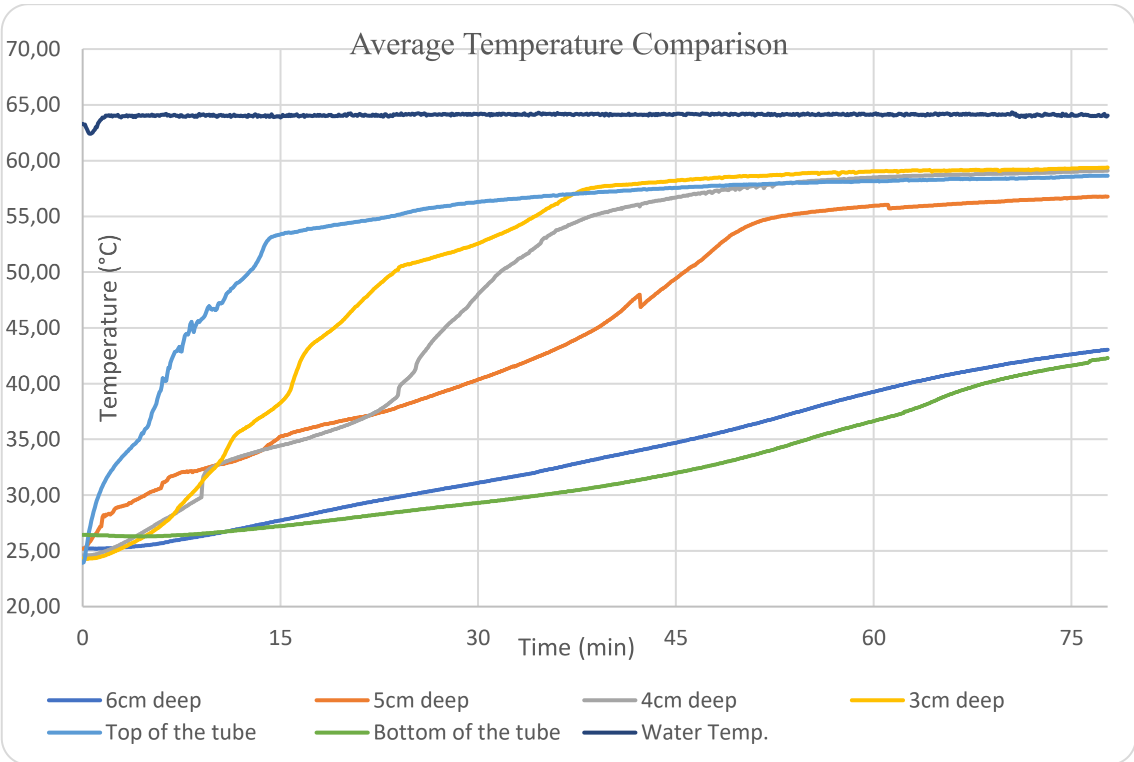

Figure 21. Average Temperature Distribution in Double Tube Centered geometry melting based on the depth of the thermocouple

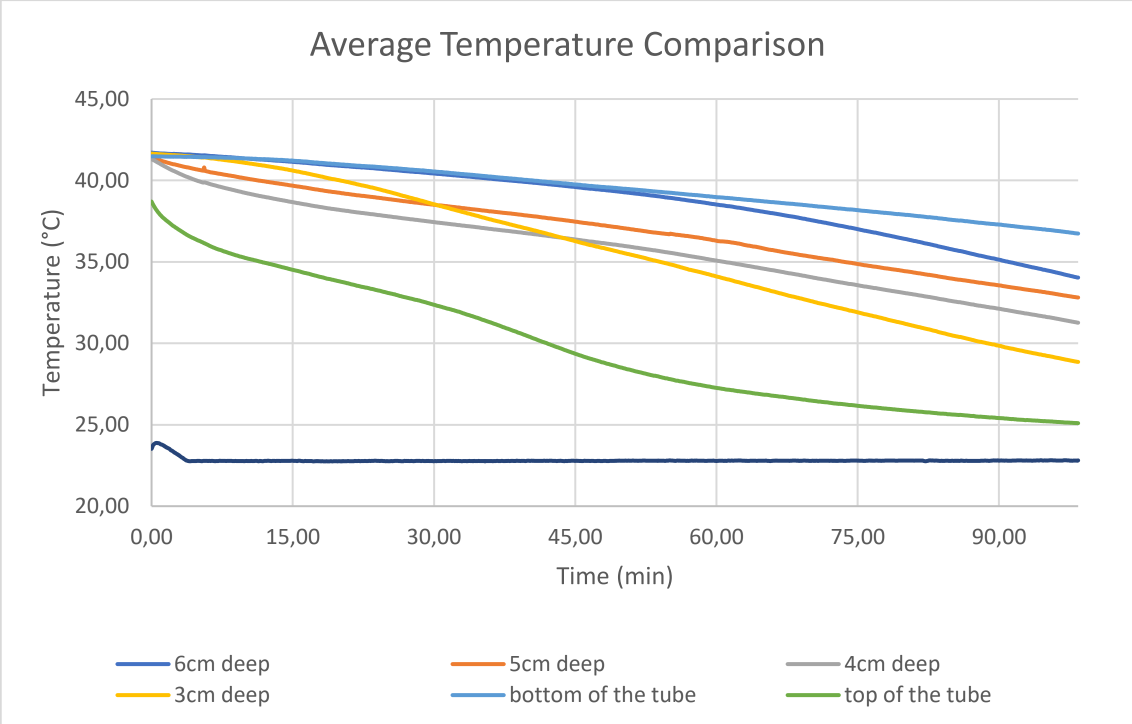

Figure 22. Average Temperature Distribution in Double Tube Centered geometry solidifying based on the depth of the thermocouple

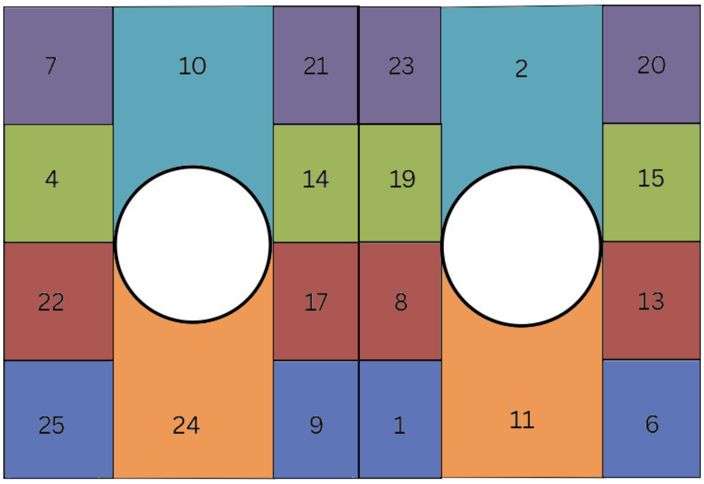

Figure 23. Thermocouple Placement for Double Tube Geometry

3.7.4 Eccentric Double-Tube Geometry

The eccentric double-tube geometry was designed to combine the advantages of increased heat transfer area and enhanced natural convection. In this configuration, two copper tubes were positioned symmetrically near the bottom region of the storage tank, with a clearance of 5 mm between the lower tube surfaces and the bottom wall. This arrangement increased the PCM volume located above the heat transfer tubes while simultaneously reducing the average conduction distance within the storage domain.

Charging experiments were conducted using water at 65°C circulating through the tube network at a constant flow rate of 2.14 L/min. Following the charging process, discharging experiments were performed to evaluate the thermal energy release characteristics of the storage unit.

Figure 24-25 presents the temperature evolution measured at different thermocouple locations during the charging and discharging processes. The recorded temperatures demonstrate the influence of eccentric tube placement and increased heat transfer area on the thermal response of the PCM domain and provide insight into the melting and solidification behavior of the storage system.

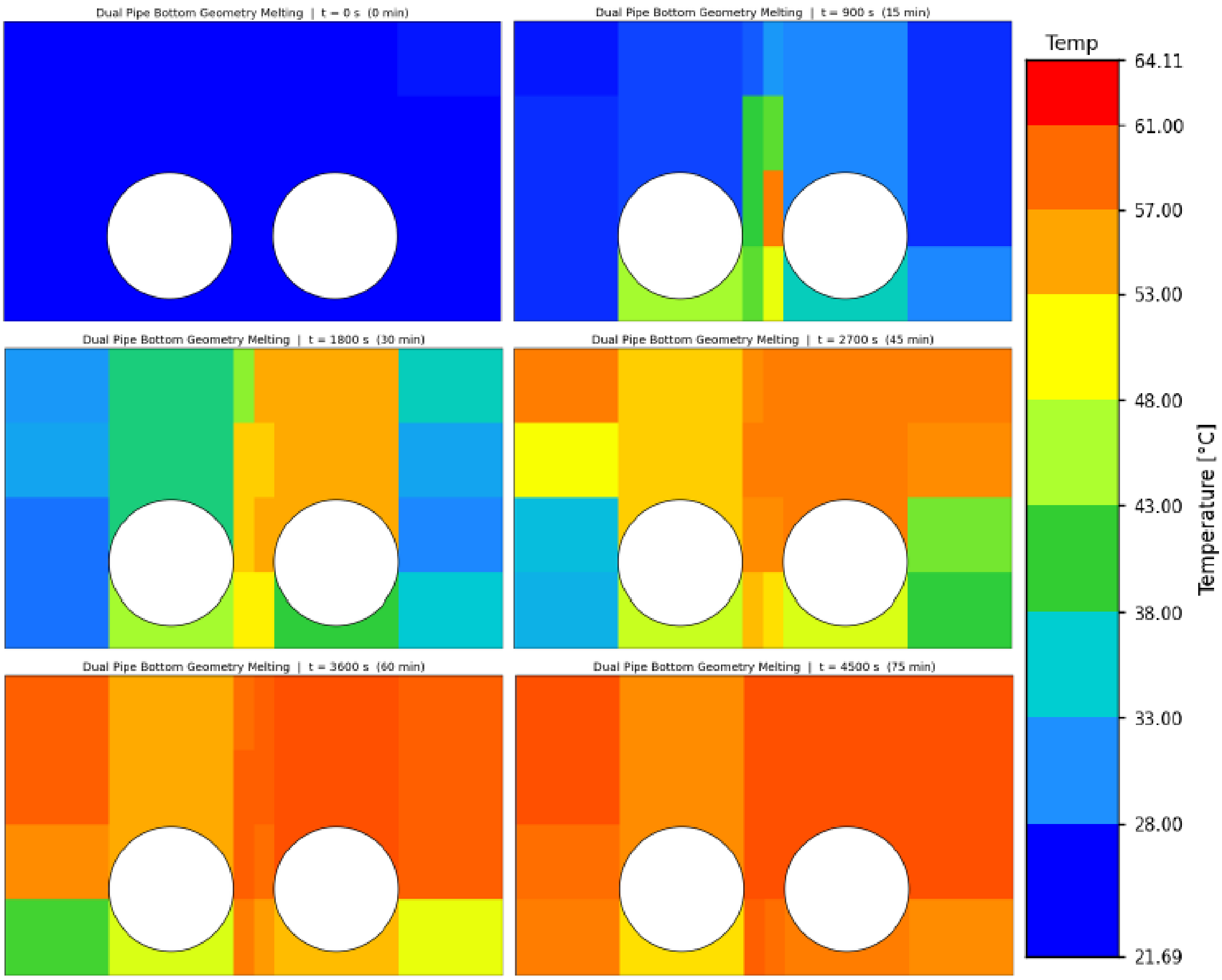

Figure 24.Melting of Double Tube Eccentric Geometry

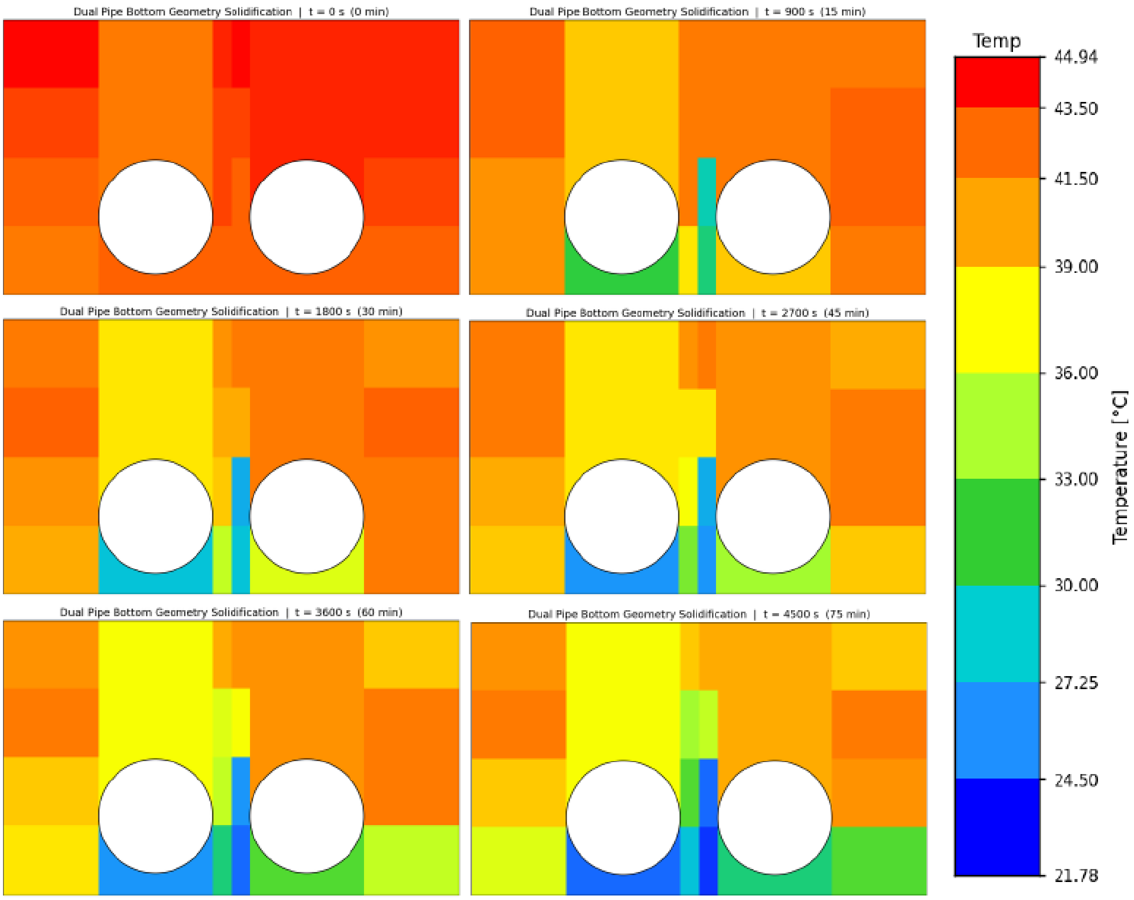

Figure 25. Solidifying of Double Tube Eccentric Geometry

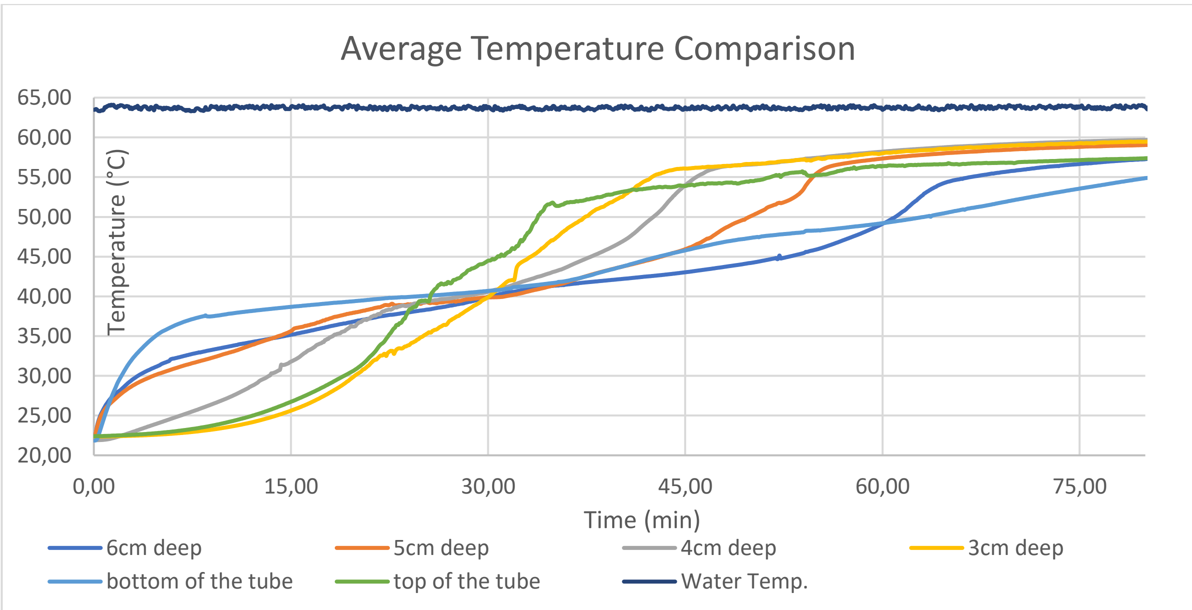

Figure 26. Average Temperature Distribution in Double Tube Eccentric geometry melting based on the depth of the thermocouple

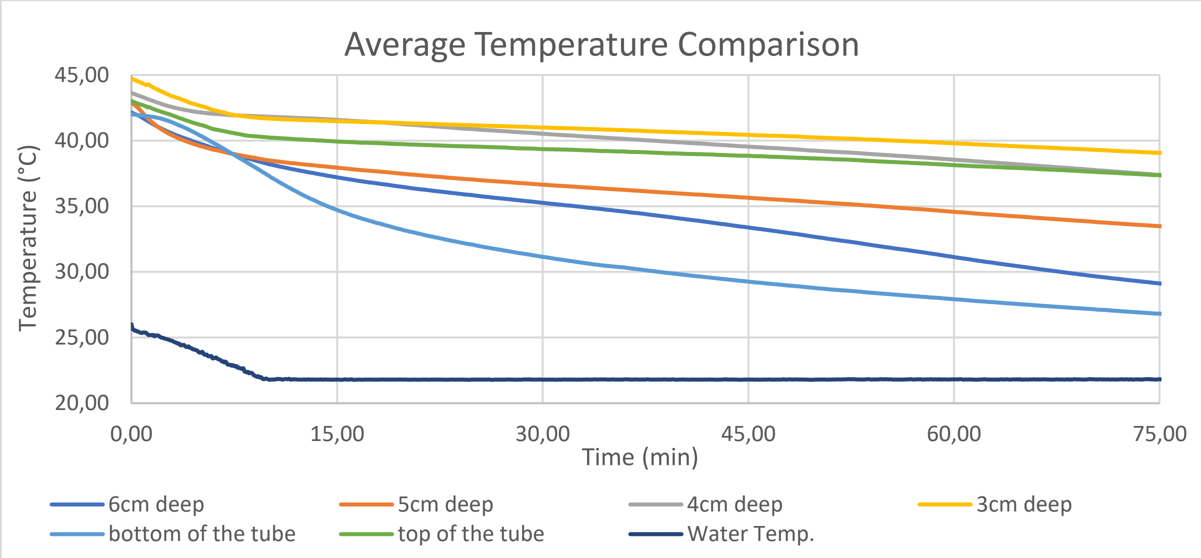

Figure 27.Average Temperature Distribution in Double Tube Eccentric geometry solidifying based on the depth of the thermocouple

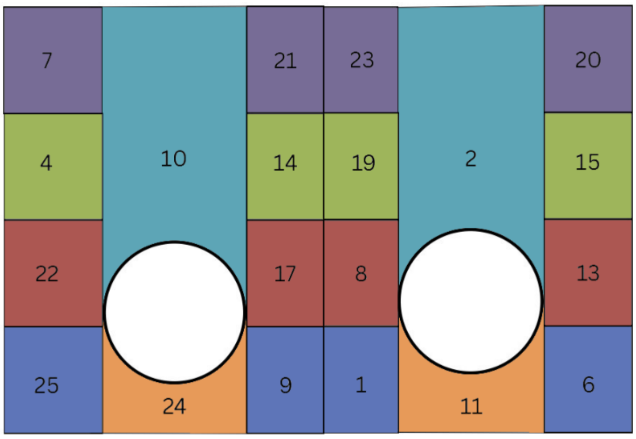

Figure 28. Thermocouple Placement for Double Tube Geometry

3.7.5 Centered Tube Geometry with Fins

The finned geometry was tested to evaluate the effect of conductive heat transfer enhancement on the melting behavior of RT42. In this configuration, a centered copper tube was equipped with three longitudinal copper fins extending along the tank depth. Two fins were positioned laterally, while one fin was directed toward the lower region of the PCM domain. Therefore, the configuration was designed to improve heat transfer especially toward the lower and side regions, where melting is generally slower in the plain centered single-tube geometry.

Figure 29 presents the melting behavior of the centered tube with fins during the charging process. Compared with the plain centered single-tube geometry, the melting front did not develop only around the circular tube surface. Instead, the fins provided additional conductive paths and transferred heat farther into the PCM domain. This behavior helped reduce the conduction-limited regions around the tube, particularly near the lower part of the tank.

The average temperature distribution shown in Figure 30 also supports the effect of the fins on the thermal response of the PCM. Since the finned geometry had the largest heat transfer area among the tested configurations, the temperature increase was distributed over a larger portion of the PCM domain. The fins improved heat transfer to the regions that were farther from the tube surface, while the open space above the tube still allowed buoyancy-driven natural convection to develop during melting.

However, the finned geometry should not be evaluated only based on heat transfer area. Although fins enhance conduction, they may also restrict the motion of the molten PCM if they occupy a large portion of the flow region. In the present design, the use of three fins created additional conductive paths without fully blocking the upper PCM region. Therefore, the finned geometry provided a balance between conduction enhancement through copper fins and natural convection development in the molten PCM.

Overall, the centered tube with fins showed improved melting behavior compared with the plain centered single-tube configuration. The main improvement was observed in the reduction of conduction-limited regions, especially around the lower and lateral parts of the PCM domain. This indicates that adding fins can be an effective method for improving the charging performance of centered tube geometries.

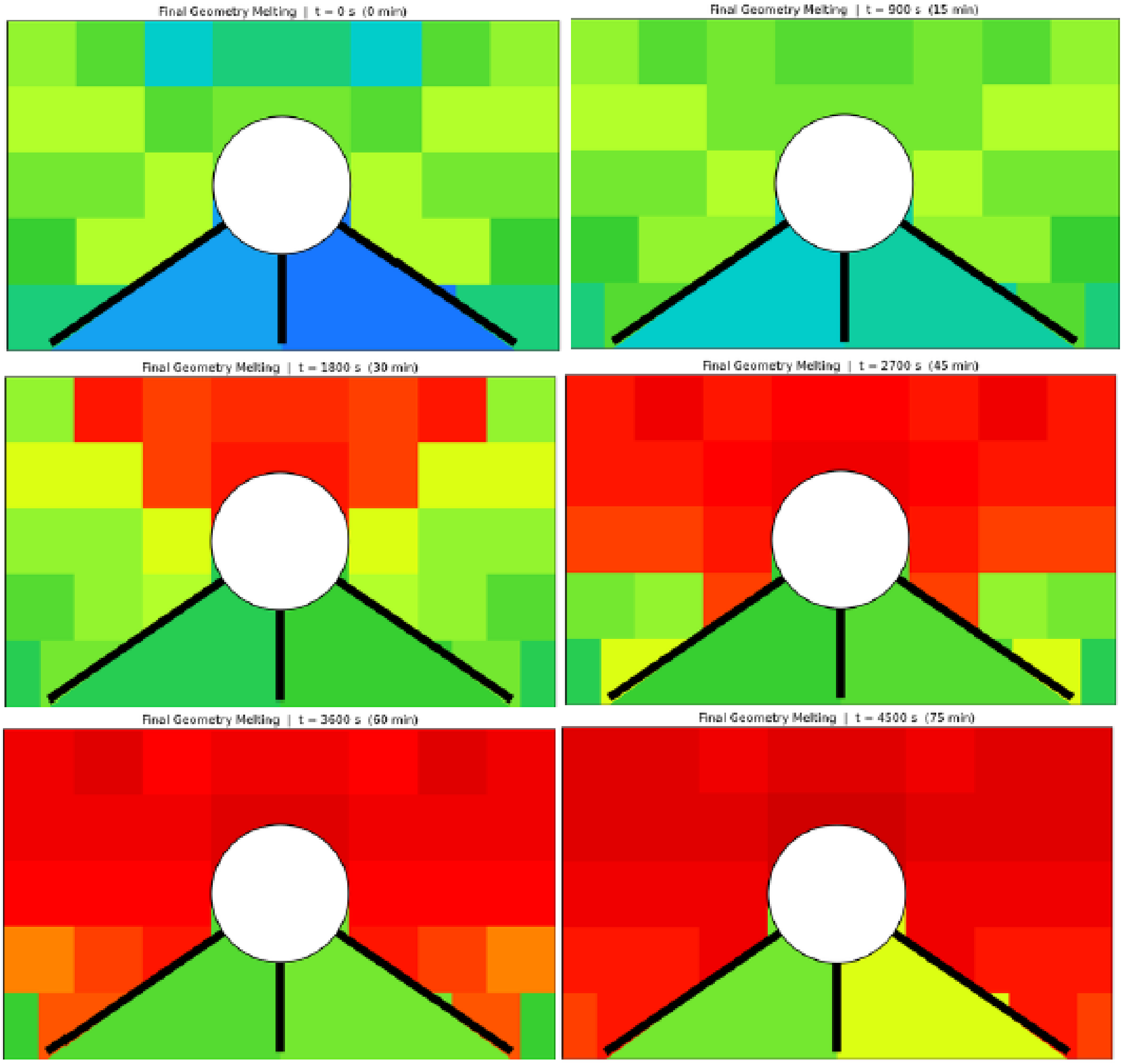

Figure 29. Melting of Centered Tube with Fins

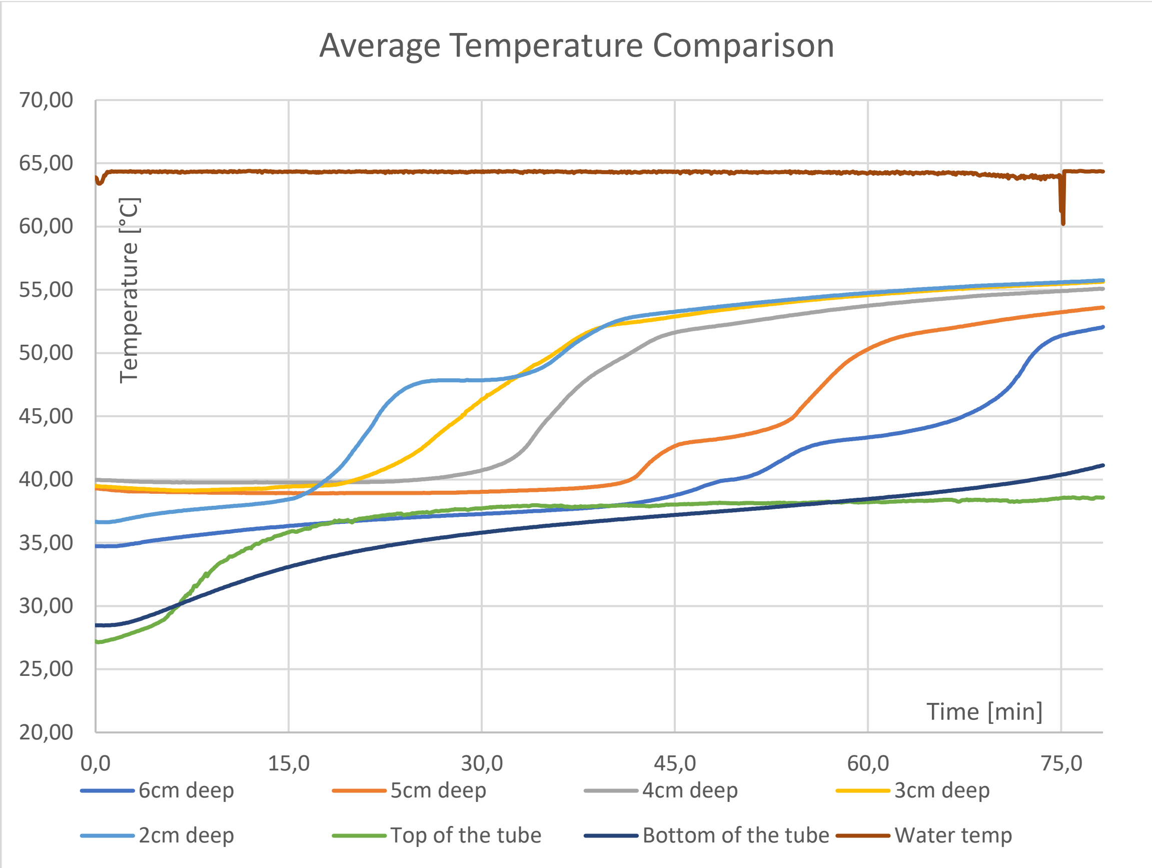

Figure 30. Average Temperature Distribution in Centered Finned geometry melting based on the depth of the thermocouple

RESULTS AND DISCUSSION

4.1 Comparison of Experimental Results

This section compares the experimental results obtained from the single-tube, double-tube and finned PCM storage tank configurations. The comparison focuses on the influence of tube position and heat transfer surface distribution on the charging and discharging behavior of RT42. During the charging experiments, water at 65°C was circulated through the copper tubes at a constant volumetric flow rate of 2.14 L/min. During the discharging experiments, the cooling HTF temperature was generally maintained at approximately 23°C under comparable flow conditions. Therefore, the observed differences between the geometries can mainly be attributed to the tube arrangement, heat transfer surface area, and the resulting heat transfer mechanisms inside the PCM domain.

4.1.1 Comparison of Single-Tube Configurations

The centered and eccentric single-tube configurations were compared to evaluate the effect of tube position on melting and solidification behavior. Both configurations had the same tank dimensions, PCM volume, tube diameter, and heat transfer surface area. Therefore, the comparison mainly represents the influence of vertical tube placement on the thermal response of the PCM.

During the melting process, the centered single-tube results shown in Figures 9–13 indicate that the PCM region above the tube heated faster than the lower region, while the bottom corners remained colder for a longer period. This behavior is mainly attributed to buoyancy-driven natural convection, which carries the melted and warmer PCM upward. In the eccentric single-tube configuration shown in Figures 14–18, the tube was positioned closer to the bottom wall; therefore, the heat source was located nearer to the lower PCM region, and the upward motion of the melted PCM contributed to a larger vertical melting region.

In the centered single-tube configuration, the tube was located at the mid-height of the PCM domain. Although this arrangement provided a symmetric heat source, the PCM located below the tube could not benefit effectively from the upward natural convection currents. As a result, the lower region and especially the bottom corners remained colder for a longer period during charging. This behavior is consistent with the temperature-depth comparison shown in Figures 11 and 12, where the lower thermocouple groups showed a slower thermal response compared with the upper regions. Since RT42 has a low thermal conductivity of approximately 0.2 W/m·K, the conduction-dominated lower region limited the overall melting uniformity.

The eccentric single-tube configuration improved the melting behavior by positioning the tube close to the bottom wall. In this geometry, the tube surface had a 5 mm clearance from the bottom wall, which corresponds to a tube center height of 19 mm from the bottom surface due to the 28 mm tube outer diameter. This placement increased the PCM volume above the heat source and allowed the buoyancy-driven flow to develop through a larger vertical region. The Rayleigh number analysis also supports this observation. The vertical characteristic length above the tube increased from 19.5 mm in the centered configuration to 34 mm in the eccentric configuration. Since the Rayleigh number is proportional to the cube of the characteristic length, this increase enhanced the natural convection potential during melting. As a result, the eccentric single-tube geometry showed a more favorable melting pattern, especially in the PCM volume above the tube.

However, the same tube placement did not provide the same advantage during solidification. In the discharging process, the PCM begins to solidify around the cooled tube surface. As the solid layer grows, liquid motion becomes limited and heat transfer becomes increasingly conduction-dominated. Under this condition, the location of the cooling surface becomes more important than the natural convection path. In the eccentric single-tube configuration, the cooling tube was located near the bottom of the tank; therefore, the thermal energy stored in the upper PCM region had to be transferred through a longer conduction path before reaching the tube surface. This delayed the cooling response of the upper PCM volume.

In contrast, the centered single-tube geometry provided a more balanced discharging behavior. Since the tube was located near the middle of the PCM domain, the maximum conduction distance from both the upper and lower regions to the cooling surface was reduced. This arrangement helped the PCM release heat more uniformly during solidification. Therefore, the single-tube comparison indicates a clear trade-off: the eccentric arrangement improves charging performance by enhancing natural convection during melting, whereas the centered arrangement provides a more balanced solidification behavior due to shorter and more symmetric conduction paths.

Overall, the eccentric single-tube geometry is more suitable when rapid charging is the main objective, while the centered single-tube geometry is more favorable when uniform discharging is prioritized.

4.1.2 Comparison of Double-Tube Configurations

The centered and eccentric double-tube configurations were compared to evaluate the effect of tube position when the heat transfer surface area was increased. In both geometries, two copper tubes were placed horizontally side by side inside the PCM tank, providing a total heat transfer area of 0.0264 m^2. In the centered double-tube configuration, the tube centers were located at the mid-height of the tank, while in the eccentric double-tube configuration, the tube centers were positioned 19 mm above the bottom surface, corresponding to a 5 mm clearance between the lower tube surfaces and the bottom wall.

During charging, the eccentric double-tube configuration showed a more favorable melting behavior because the heat sources were located closer to the bottom region and a larger PCM volume remained above the tubes. This promoted buoyancy-driven upward flow and supported the development of the melting front through a larger vertical region. In contrast, the centered double-tube configuration still left the PCM below the tubes more dependent on conduction, which caused slower heating in the lower region.

During discharging, the centered double-tube configuration provided a more balanced cooling behavior. Since the tubes were located closer to both the upper and lower PCM regions, the maximum conduction distance was reduced. In the eccentric double-tube configuration, the upper PCM region was farther from the cooling surfaces, which delayed heat removal from the upper part of the tank.

Overall, the eccentric double-tube geometry was more advantageous for charging, while the centered double-tube geometry provided a more uniform discharging behavior.

4.1.3 Comparison of Centered Single-Tube, Centered Double-Tube, and Finned Geometries

The centered single-tube, centered double-tube, and centered finned geometries were compared to evaluate how heat transfer surface area and heat source distribution affect the charging behavior of RT42. Since all three configurations were centered, the comparison mainly focuses on the effect of increasing the heat transfer area and modifying the heat transfer path, rather than the effect of tube eccentricity.

Table 13. Heat Transfer Surface Area Comparison of Centered Geometries

Geometry	Configuration	Heat Transfer Surface Area (m^2)	Relative Area Compared with Centered Single-Tube
G1	Centered Single-Tube	0.0132	1.00
G3	Centered Double-Tube	0.0264	2.00
G5	Centered Tube with Fins	0.0435	3.30

As shown in Table 13, the centered double-tube geometry doubled the heat transfer surface area compared with the centered single-tube geometry. The finned geometry provided the largest heat transfer area, approximately 3.3 times higher than the centered single-tube configuration. Therefore, the comparison between these three centered geometries clearly shows how increasing the effective heat transfer area improves the thermal interaction between the HTF and the PCM.

From the perspective of melting behavior, the centered single-tube geometry had the weakest performance among the three because heat transfer was concentrated around one tube and the lower region remained conduction-dominated. The centered double-tube geometry improved the overall heat distribution by creating two melting regions and reducing the PCM-to-tube distance. The finned geometry further enhanced heat transfer by extending the conductive surface into the PCM, which helped the lower and side regions heat more effectively.

Overall, the comparison shows that increasing the heat transfer area improves the charging performance of centered geometries. The centered double-tube design improves melting mainly by distributing the heat source, while the finned geometry improves melting by extending conductive heat transfer paths into the PCM. Therefore, among the centered configurations, the finned geometry provides the strongest improvement for conduction-limited regions, whereas the centered double-tube geometry provides a more distributed heat source arrangement.

4.2 Cost analysis of the project

The cost analysis was prepared to estimate the total expenditure required for the manufacturing, assembly, and testing of the PCM-based thermal energy storage system. The main cost items were PCM material, tank materials and manufacturing, pipes, insulation, adapters, chain components, and miscellaneous assembly materials.

The total estimated cost of the project was calculated as ₺11,750. Some components, such as the oil pump, DC motor, valve, thermal oil, thermocouples, and datalogger, were already available in the laboratory or supplied without additional cost. Therefore, these items were listed as ₺0 on the cost table.

This cost analysis represents the prototype-scale experimental setup. Since labor cost, machining time, and the full market price of borrowed laboratory equipment were not included, the actual cost of reproducing the complete system may be higher than the estimated value.

Table 14. Cost Analysis

Component	Quantity	Total Cost
Oil pump	1	₺0
24V DC motor	1	₺0
Thermal oil	2L	₺0
PCM material	7 kg	₺3000
Pipes	7 m	₺1500
Valve	1	₺0
Adapters	2	₺500
Thermocouples	30	₺0
Datalogger	1	₺0

Tank materials / manufacturing	6	₺4000
Insulation material	4	₺1000
Chain	5 m	₺1250
Miscellaneous	-	₺500
Total Estimated Cost		₺11750

4.3 Lessons Learned

One of the main lessons learned during this project was that experimental studies can involve many unexpected difficulties beyond theoretical calculations and design assumptions. Although the system was designed based on engineering calculations and literature knowledge, several practical issues occurred during the experimental process. These included PCM leakage, sealing problems, material compatibility issues, delays in material supply and shipping, cost limitations, and unexpected problems during manufacturing and assembly.

These challenges showed that effective time management is as important as technical design in experimental engineering projects. Some problems, such as leakage and material incompatibility, required additional testing, redesign, and troubleshooting. Therefore, allocating more time for unexpected failures, procurement delays, and repeated experimental trials would have made the project process more efficient and less constrained.

In addition to the technical knowledge gained about PCM behavior, heat transfer mechanisms, natural convection, and storage tank geometry, the project also provided important practical experience. The experimental stage improved our ability to think quickly, identify problems, and develop engineering solutions under time and resource limitations. As a result, this project contributed not only to our technical understanding of latent thermal energy storage systems, but also to our project management, decision-making, and problem-solving skills.

4.4 For Future Improvements

4.4.1 Controlled HTF Storage Tank Design for Solar Integration

For future studies, the heat transfer fluid storage system used in the solar-integrated setup can be improved by redesigning the HTF storage tank as a shell-and-tube type thermal control unit. In the present solar integration concept, thermal oil is heated by the parabolic dish collector and then circulated through the PCM storage unit. However, unlike the laboratory-scale water bath experiments, solar radiation is not constant during outdoor operation. Variations in solar intensity, wind conditions, cloud cover, and collector alignment can cause continuous fluctuations in the HTF temperature. These fluctuations may lead to unstable inlet temperature conditions and reduce the repeatability of the PCM charging experiments.

A shell-and-tube type HTF storage tank can be used to improve the thermal stability of the solar-driven system. In this design, the hot thermal oil can be stored or circulated on one side of the tank, while a secondary cooling fluid, such as water, can be circulated through the other side using a circulator. When the oil temperature rises above the desired operating range, the cooling water can remove excess heat from the system. In this way, the HTF temperature can be maintained closer to the target value before it enters the PCM storage tank.

This improvement would provide better control over the boundary conditions of the experiment. Since PCM melting behavior is strongly affected by the inlet HTF temperature, maintaining a stable HTF temperature is essential for reliable comparison between different PCM geometries. A controlled shell-and-tube HTF storage tank would reduce temperature overshoot, prevent uncontrolled overheating of the oil, and allow the system to operate under more repeatable thermal conditions. Therefore, this modification would make the solar-integrated experimental setup more suitable for systematic performance evaluation.

4.4.2 Improved Solar Tracking Mechanism

Another important improvement can be made in the solar tracking mechanism of the parabolic dish collector. Parabolic dish collectors concentrate solar radiation onto a focal region, and their thermal performance strongly depends on the alignment between the collector and the sun. If the dish is not properly oriented, the concentrated radiation may shift away from the heating region, reducing the energy transferred to HTF. Therefore, even small angular deviations can cause significant variations in the oil temperature during outdoor experiments.

To improve the stability of the solar input, a gear-based tracking mechanism can be implemented. Instead of adjusting the collector manually, the dish can be moved gradually and more precisely using a gear system connected to a motor. A geared mechanism would allow smoother angular motion and better control of the collector orientation throughout the day. This would help keep the focal point closer to the HTF heating region for a longer period and reduce sudden changes in heat input.

In addition, the tracking system can be further improved by integrating a simple control system based on time, solar position, or light sensors. With such a system, the collector could follow the sun more accurately and maintain a more stable thermal input to the oil tank. As a result, the HTF temperature would become more consistent, and the solar charging experiments would be less affected by manual adjustment errors. This improvement would increase the reliability of the solar-integrated PCM storage system and make the experimental results more comparable with controlled laboratory tests.

4.4.3 Larger-Scale PCM Domain and System Optimization

Future experiments can also be performed with larger PCM domains to evaluate the scalability of the geometries investigated. In the present study, the PCM storage tanks were designed at laboratory scale with approximately constant PCM volume, which allowed a fair comparison between different tube arrangements and fin configurations. However, real thermal energy storage applications generally require larger PCM volumes and longer operating times. Therefore, testing larger-scale PCM domains would provide more realistic information about the practical performance of the proposed designs.

Increasing the PCM domain size would make it possible to examine how melting front development, natural convection, and temperature stratification change at larger scales. In small-scale tanks, heat transfer distances are limited, and the melting process can be observed within relatively short time periods. In larger systems, however, conduction limitations may become more significant, and natural convection patterns may develop differently. Therefore, scaling up the system would help determine whether the advantages of eccentric tube placement, double-tube configurations, and finned geometries remain effective for larger storage units.

Further system-level improvements can also be implemented to increase the reliability and accuracy of future experiments. Better thermal insulation can be applied to reduce heat losses from the tank and piping system. Additional thermocouples can be placed in critical regions, especially near the bottom corners, around the fins, and close to the tube surfaces, to obtain a more detailed temperature distribution. Moreover, automated temperature and flow control systems can be used to maintain stable experimental conditions during both charging and discharging processes.

Overall, increasing the PCM domain size and improving the experimental control system would provide a more realistic evaluation of the thermal storage performance. These improvements would also make it possible to better assess the applicability of the proposed PCM geometries for future solar thermal energy storage systems.

CONCLUSION

In this project, the effect of PCM domain geometry on the thermal performance of latent thermal energy storage systems was investigated experimentally using RT42 paraffin as the phase change material. Five different storage configurations – centered single-tube, eccentric single-tube, centered double-tube, eccentric double-tube, and centered finned geometries – were designed, manufactured, and tested under an identical PCM volume and comparable operating conditions. Keeping the PCM volume constant ensured that the observed differences could be attributed mainly to tube position and heat transfer surface distribution rather than to the storage material or the charging and discharging conditions.

The experimental results showed that the position of the heat transfer tube has a strong and direction-dependent influence on the charging and discharging behavior of the PCM. During melting (charging), the eccentric configurations consistently performed better than the centered ones. Lowering the tube toward the bottom of the tank increased the PCM volume above the heat source and enlarged the vertical characteristic length, which raised the Rayleigh number and strengthened buoyancy-driven natural convection, producing a faster and more uniform melting front. During solidification (discharging), the trend was reversed. As the solid layer grows, heat transfer becomes conduction-dominated, and the centered configurations provided shorter and more symmetric conduction paths between the PCM and the cooling surface, resulting in a more balanced discharging behavior. Both the single-tube and double-tube comparisons confirmed this trade-off: the eccentric arrangement is preferable when rapid charging is the priority, whereas the centered arrangement is preferable when uniform discharging is required.

The comparison of the centered single-tube, centered double-tube, and finned geometries showed that increasing the effective heat transfer area significantly improves charging performance. Doubling the surface area with a second tube and increasing it by roughly 3.3 times with fins both reduced the conduction-limited regions of the PCM domain, which is particularly important given the low thermal conductivity of RT42 (approximately 0.2 W/m·K). Among the centered geometries, the finned configuration provided the strongest improvement for the conduction-limited lower and lateral regions, while the centered double-tube configuration improved melting mainly by distributing the heat source more evenly throughout the domain.

Overall, the study confirmed that geometry optimization is an effective way to enhance the performance of latent thermal energy storage systems without modifying the storage material itself. No single geometry was optimal for both processes; the most suitable configuration depends on whether charging or discharging performance is prioritized, and combining eccentric tube placement with extended (finned) surfaces offers a promising route to improving both the heat transfer area and natural convection simultaneously. Despite practical challenges such as PCM leakage and sealing problems, the project was completed within the planned schedule, and the prototype-scale system was realized at an estimated cost of ₺11,750.

Finally, the experimental work provided a solid basis for the planned solar integration phase of the project. The findings on tube position, heat transfer area, and natural convection can be applied directly to the design of the parabolic-dish-driven PCM storage unit. Future work should focus on stabilizing the heat transfer fluid temperature through a controlled shell-and-tube storage tank, improving the accuracy of the solar tracking mechanism, and scaling up the PCM domain to assess whether the observed advantages of eccentric and finned geometries remain effective in larger and more realistic thermal energy storage systems.

REFERENCES

[1] Ali, F. H., Al-amir, Q. R., Hamzah, H. K., & Alahmer, A. (2025). Integrating thermal phase-change material energy storage with solar collectors: A comprehensive review of techniques and applications. *International Communications in Heat and Mass Transfer, 162*, 108606. https://doi.org/10.1016/j.icheatmasstransfer.2025.108606

[2] Tajik Jamal-Abad, M., Cortés, C., Martínez, A., & Carmona, M. (2025). Numerical investigation of the effect of the mushy zone parameter and the thermal properties of paraffin-based PCMs on solidification modeling under T-history conditions. Energy Storage, 7, e70130. https://doi.org/10.1002/est2.70130

[3] Demirkıran, İ. G., & Cetkin, E. (2021). Emergence of rectangular shell shape in thermal energy storage applications: Fitting melted phase changing material in a fixed space. *Journal of Energy Storage, 37*, 102455. https://doi.org/10.1016/j.est.2021.102455

[4] Demirkıran, İ. G., Niedermeier, K., & Çetkin, E. (2025). Hollowed and perforated fins in latent heat storage units for high-temperature hybrid thermal energy storage applications. *Energy Conversion and Management, 340*, 119998. https://doi.org/10.1016/j.enconman.2025.119998

[5] Rahman, I. U., Khan, N., Manca, O., Buonomo, B., & Nardini, S. (2025). Experimental thermal analysis of box-type shell-and-tube configuration filled with RT42 phase change material: A case study. *Physchem*, *5*, Madde 39. https://doi.org/10.3390/physchem5040039

[6] https://www.coralinnovative.com/

APPENDIX

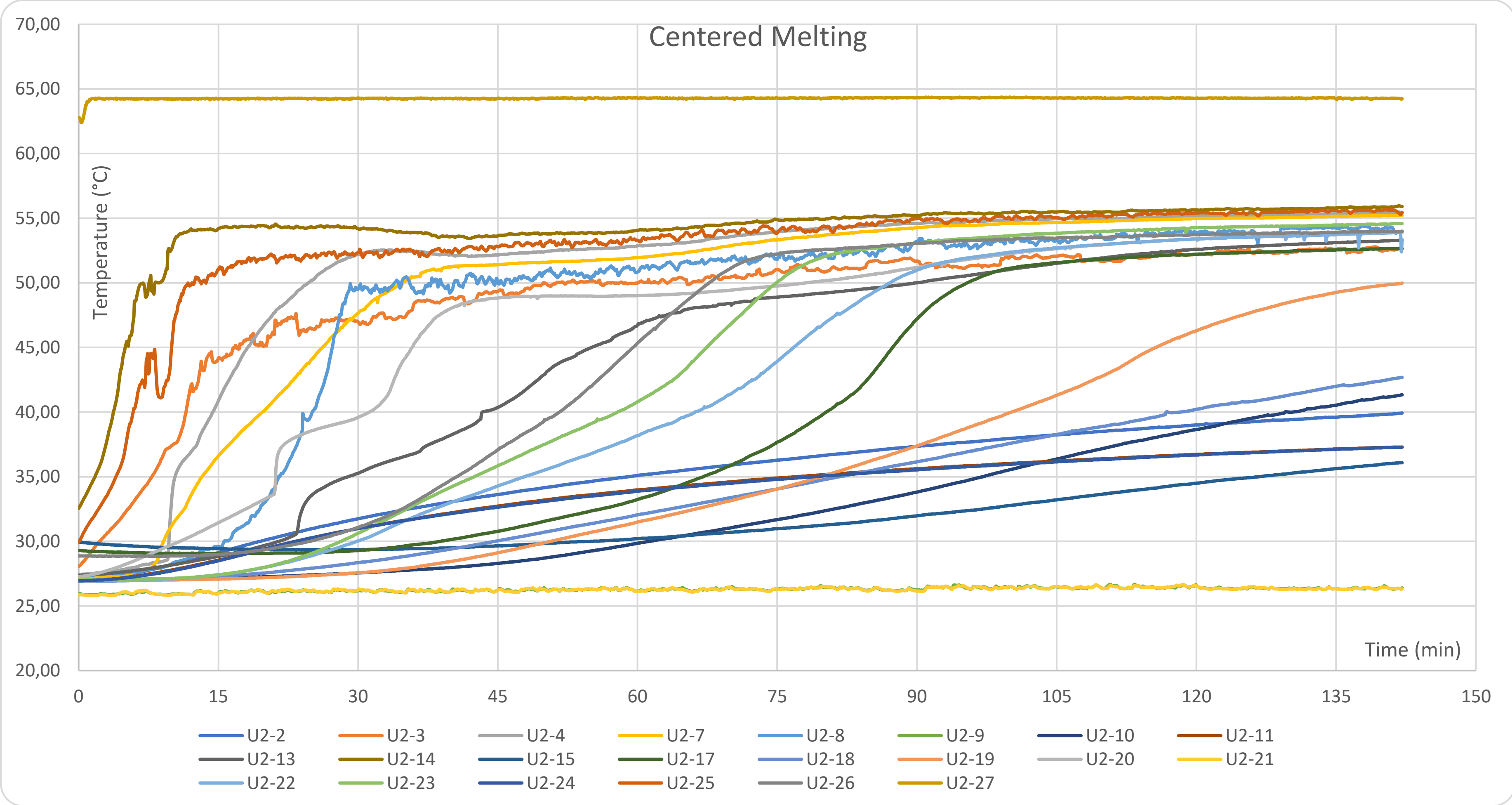

Centered Melting
Temperature (°C)
70,00
65,00
60,00
55,00
50,00
45,00
40,00
35,00
30,00
25,00
20,00
0
15
30
45
60
75
90
105
120
135
150
Time (min)
U2-2
U2-3
U2-4
U2-7
U2-8
U2-9
U2-10
U2-11
U2-13
U2-14
U2-15
U2-17
U2-18
U2-19
U2-20
U2-21
U2-22
U2-23
U2-24
U2-25
U2-26
U2-27

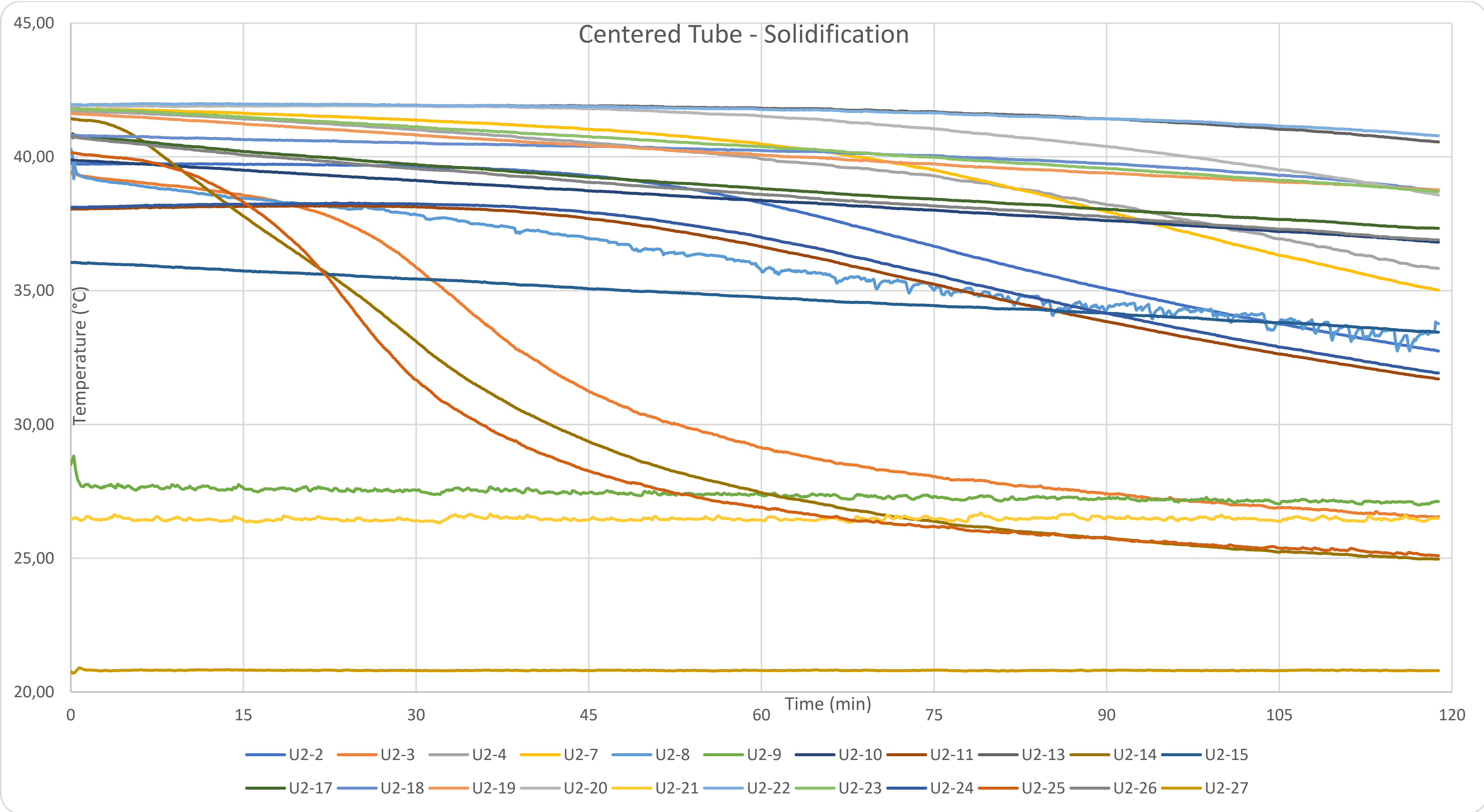
Centered Tube - Solidification
Temperature (°C)
Time (min)
45,00
40,00
35,00
30,00
25,00
20,00
0
15
30
45
60
75
90
105
120
U2-2
U2-3
U2-4
U2-7
U2-8
U2-9
U2-10
U2-11
U2-13
U2-14
U2-15
U2-17
U2-18
U2-19
U2-20
U2-21
U2-22
U2-23
U2-24
U2-25
U2-26
U2-27

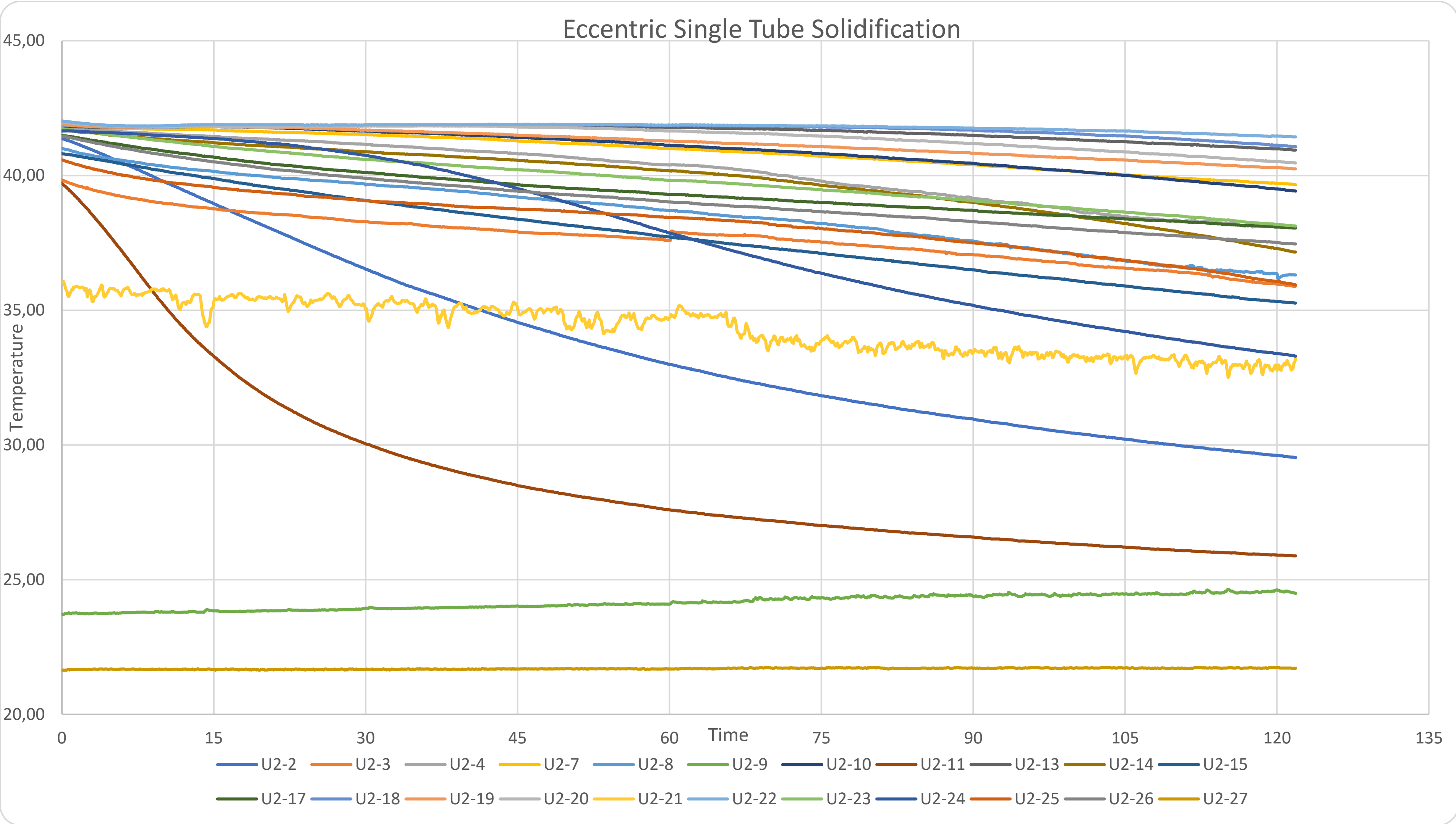

Eccentric Single Tube Solidification
45,00
40,00
35,00
30,00
25,00
20,00
Temperature
0
15
30
45
60
75
90
105
120
135
Time
U2-2
U2-3
U2-4
U2-7
U2-8
U2-9
U2-10
U2-11
U2-13
U2-14
U2-15
U2-17
U2-18
U2-19
U2-20
U2-21
U2-22
U2-23
U2-24
U2-25
U2-26
U2-27

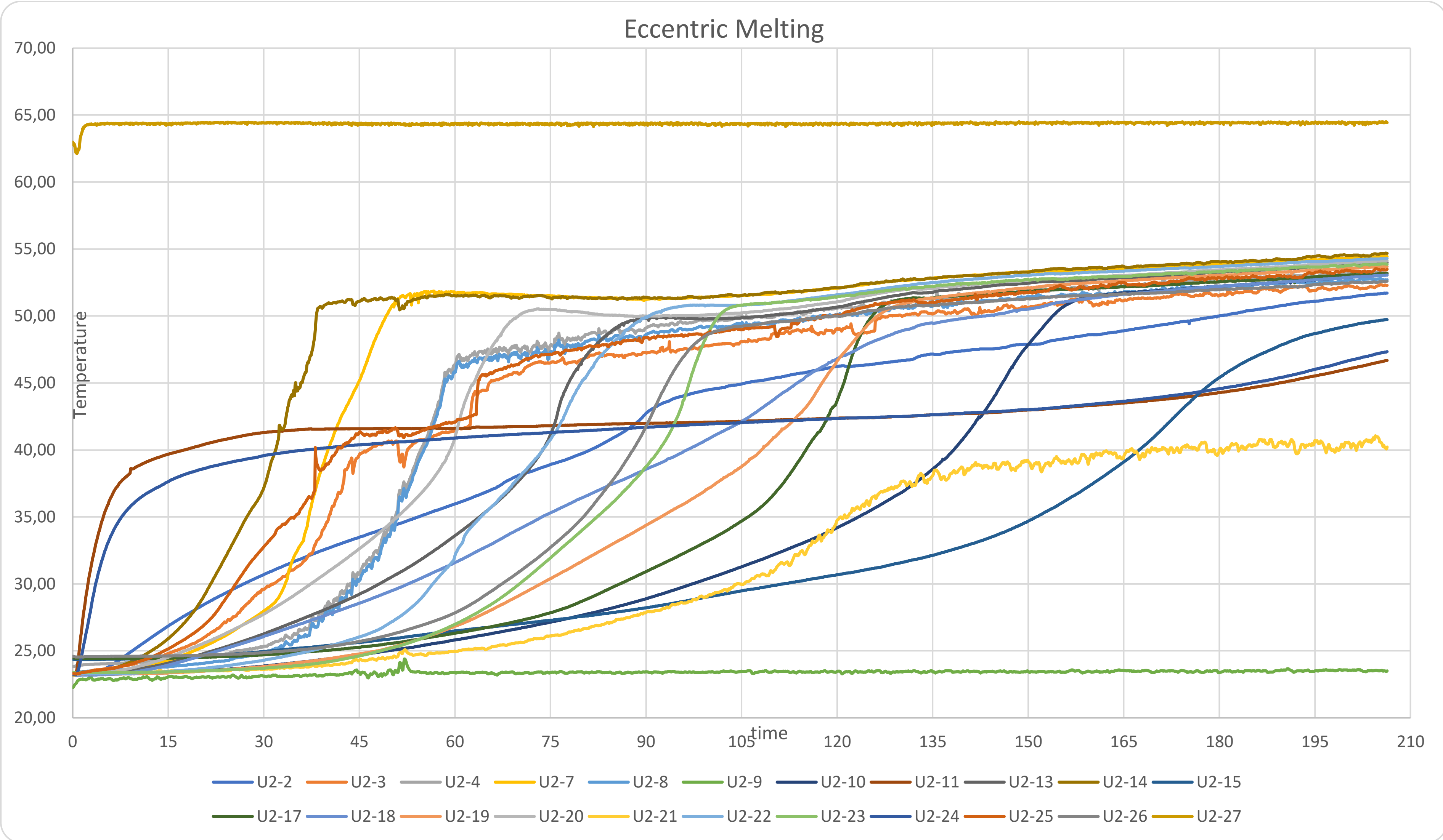

Eccentric Melting
70,00
65,00
60,00
55,00
50,00
45,00
40,00
35,00
30,00
25,00
20,00
Temperature
0
15
30
45
60
75
90
105
120
135
150
165
180
195
210
time
U2-2
U2-3
U2-4
U2-7
U2-8
U2-9
U2-10
U2-11
U2-13
U2-14
U2-15
U2-17
U2-18
U2-19
U2-20
U2-21
U2-22
U2-23
U2-24
U2-25
U2-26
U2-27

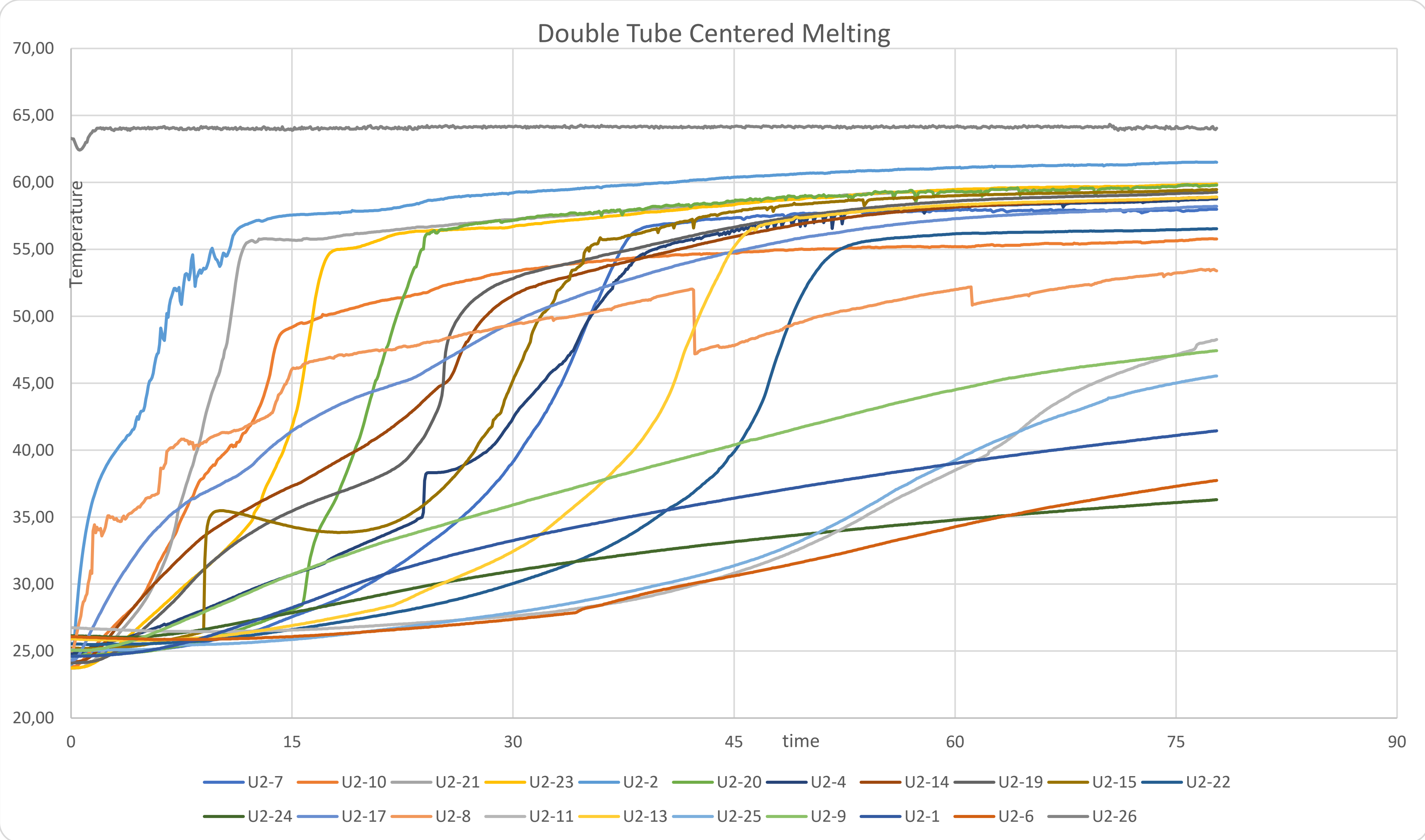

Double Tube Centered Melting
Temperature
70,00
65,00
60,00
55,00
50,00
45,00
40,00
35,00
30,00
25,00
20,00
0
15
30
45
time
60
75
90
U2-7
U2-10
U2-21
U2-23
U2-2
U2-20
U2-4
U2-14
U2-19
U2-15
U2-22
U2-24
U2-17
U2-8
U2-11
U2-13
U2-25
U2-9
U2-1
U2-6
U2-26

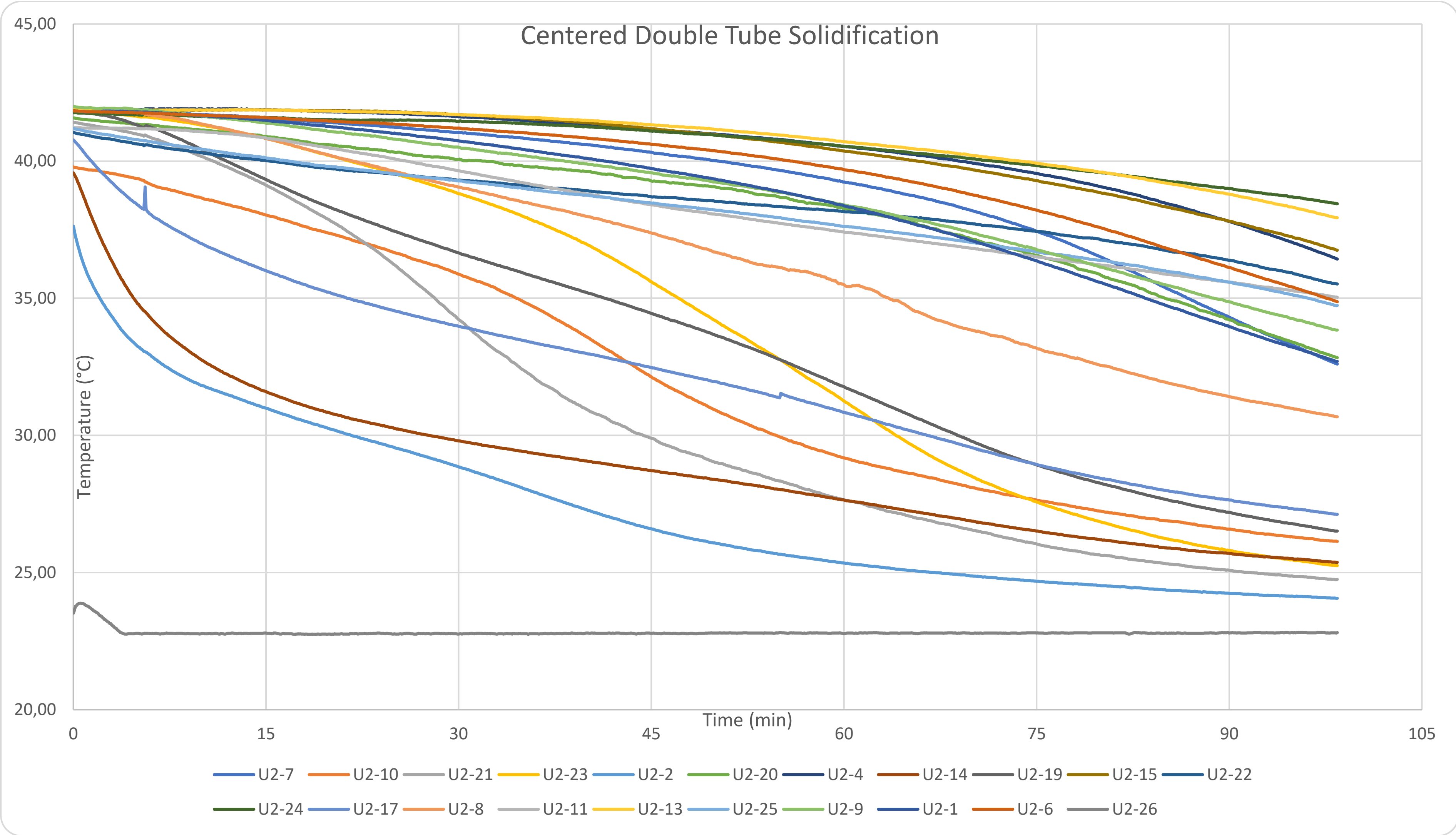

Centered Double Tube Solidification
45,00
40,00
35,00
30,00
25,00
20,00
Temperature (°C)
0
15
30
45
60
75
90
105
Time (min)
U2-7
U2-10
U2-21
U2-23
U2-2
U2-20
U2-4
U2-14
U2-19
U2-15
U2-22
U2-24
U2-17
U2-8
U2-11
U2-13
U2-25
U2-9
U2-1
U2-6
U2-26

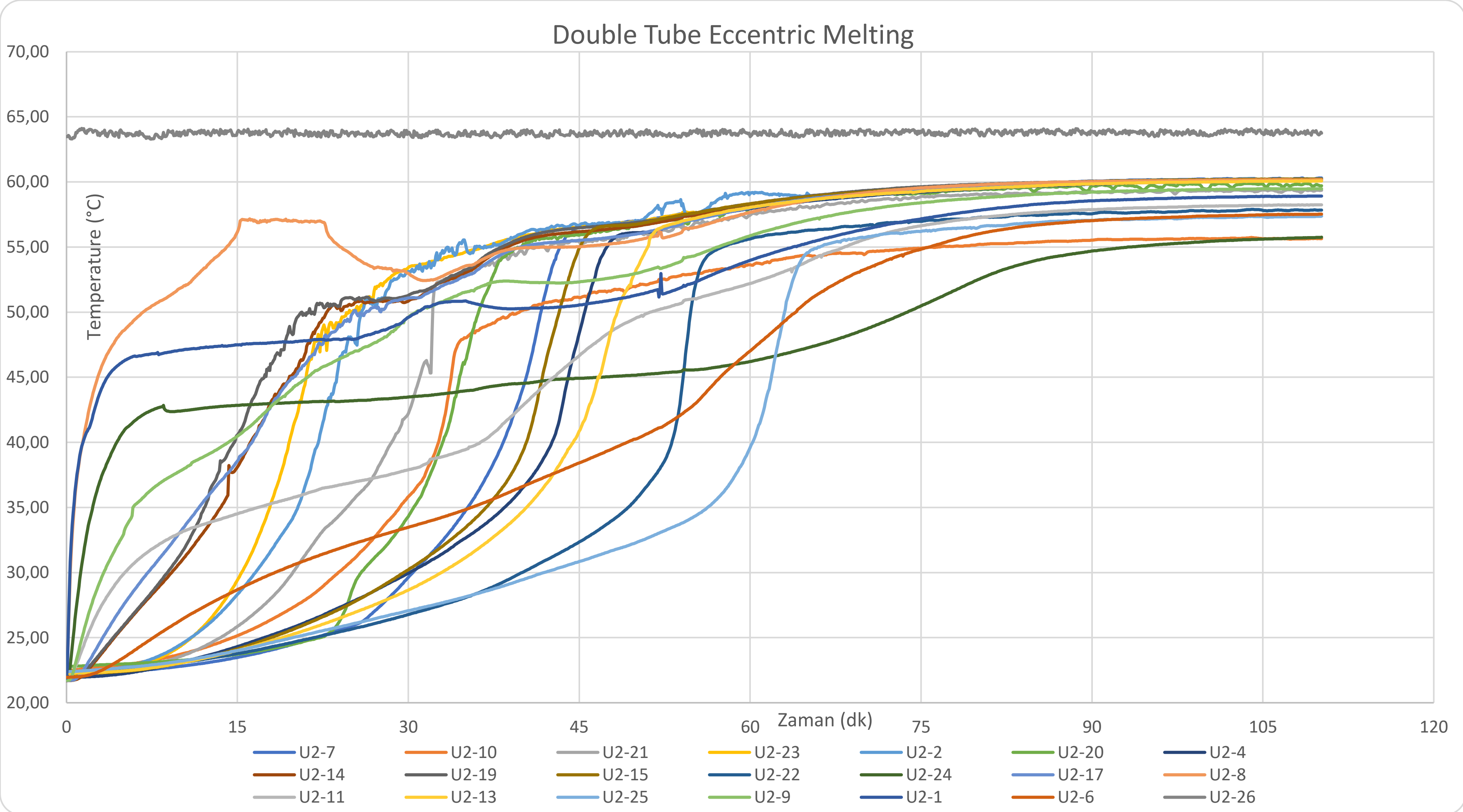
Double Tube Eccentric Melting
Temperature (°C)
Zaman (dk)
70,00
65,00
60,00
55,00
50,00
45,00
40,00
35,00
30,00
25,00
20,00
0
15
30
45
60
75
90
105
120
U2-7
U2-10
U2-21
U2-23
U2-2
U2-20
U2-4
U2-14
U2-19
U2-15
U2-22
U2-24
U2-17
U2-8
U2-11
U2-13
U2-25
U2-9
U2-1
U2-6
U2-26

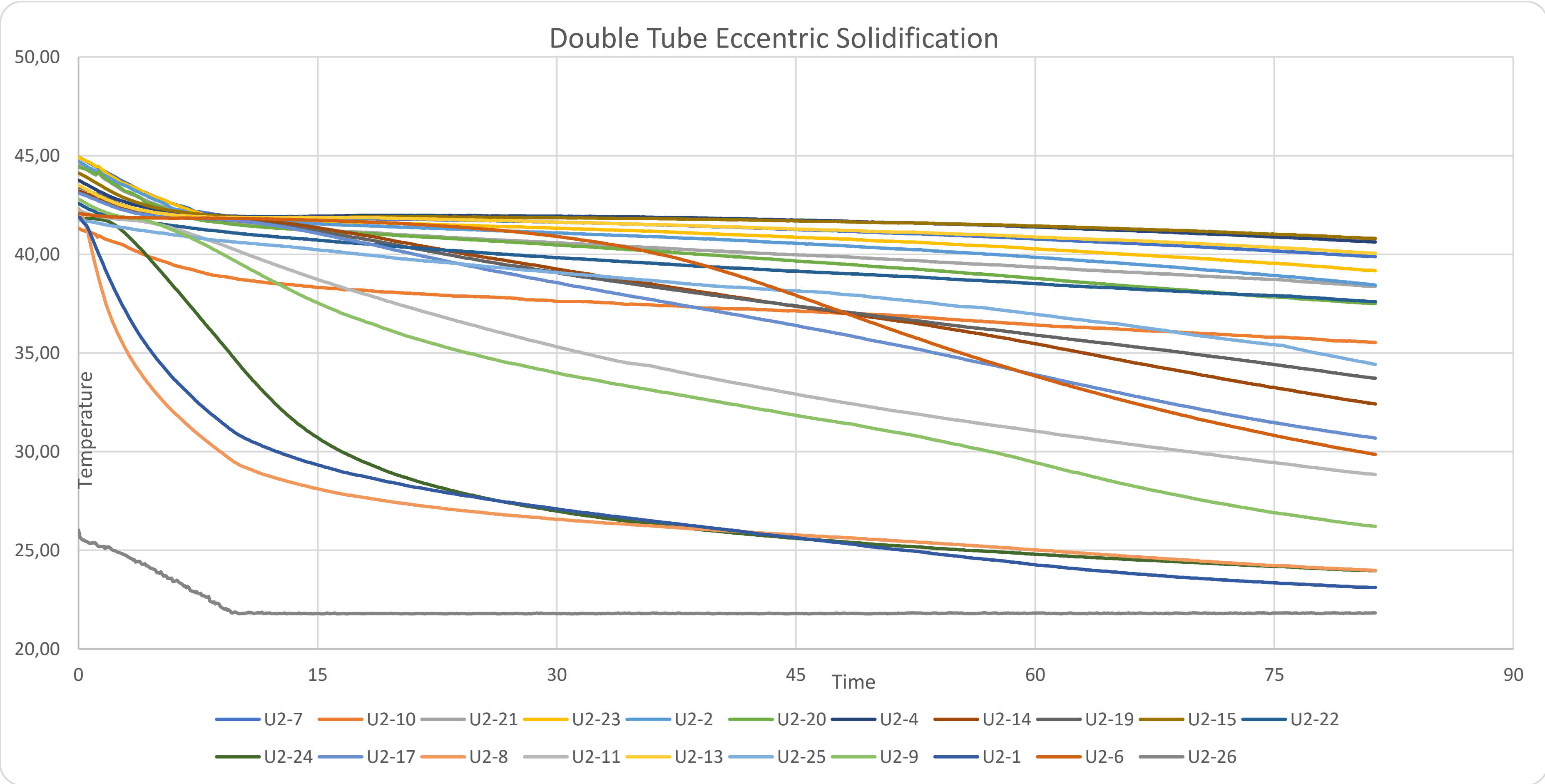

Double Tube Eccentric Solidification
50,00
45,00
40,00
35,00
30,00
25,00
20,00
Temperature
0
15
30
45
60
75
90
Time
U2-7
U2-10
U2-21
U2-23
U2-2
U2-20
U2-4
U2-14
U2-19
U2-15
U2-22
U2-24
U2-17
U2-8
U2-11
U2-13
U2-25
U2-9
U2-1
U2-6
U2-26

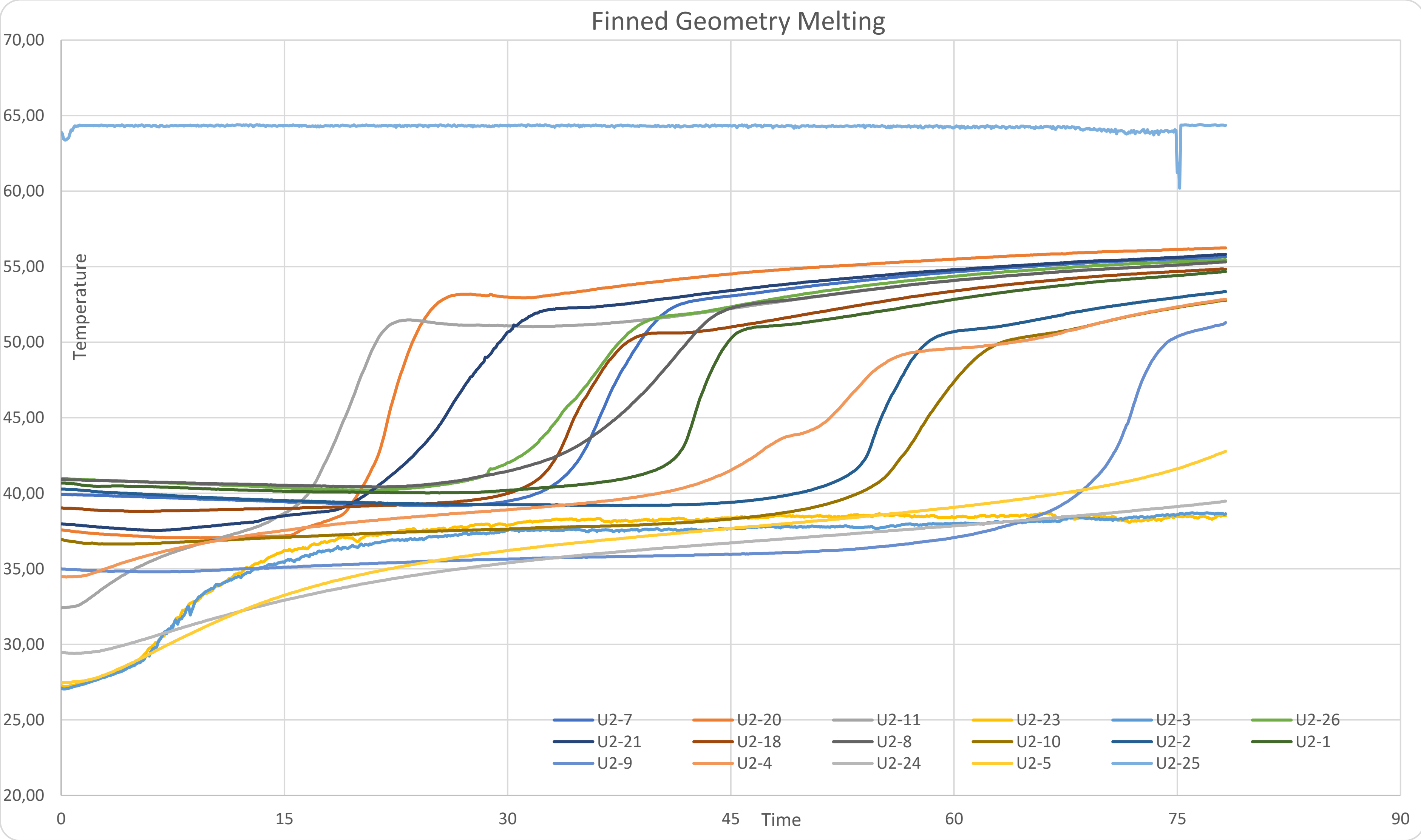

Finned Geometry Melting
70,00
65,00
60,00
55,00
50,00
45,00
40,00
35,00
30,00
25,00
20,00
Temperature
0
15
30
45
Time
60
75
90
U2-7
U2-20
U2-11
U2-23
U2-3
U2-26
U2-21
U2-18
U2-8
U2-10
U2-2
U2-1
U2-9
U2-4
U2-24
U2-5
U2-25

https://drive.google.com/drive/folders/1qpOND0HTYEnMRHEt9JZ0R_isXoquxibN?usp=drive_link

Presentation Number	Workpackages (WP)	Weight of WP	Gamze Uyaroğlu	Eren Meydan
Presentation 1	Literature Survey	30	15	15
	Preliminary Calculations	35	15	20
	Conseptual Design	35	20	15
	Subtotal	**100**	**50**	**50**
Presentation Number	**Workpackages (WP)**	**Weight of WP**	**Gamze Uyaroğlu**	**Eren Meydan**
Presentation 2	CAD Design	30	30	0
	Manufacturing	30	0	30
	Marketing and Purchase	20	10	10
	Experimental setup	20	10	10
	Subtotal	**100**	**50**	**50**
Presentation Number	**Workpackages (WP)**	**Weight of WP**	**Gamze Uyaroğlu**	**Eren Meydan**
Presentation 3	Test Setup and Preperation	20	10	10
	Experimental Execution	40	25	15

	Data Acquisition and Analaysis	20	0	20
	Performance Evaluation and Calibration	20	15	5
	Subtotal	**100**	**50**	**50**
Presentation Number	**Workpackages (WP)**	**Weight of WP**	**Gamze Uyaroğlu**	**Eren Meydan**
Presentation 4	Test Setup and Preperation	20	10	10
	Experimental Execution	40	20	20
	System Verification	10	10	0
	Performance Evaluation and Calibration	30	10	20
	Subtotal	**100**	**50**	**50**
Presentation Number	**Workpackages (WP)**	**Weight of WP**	**Gamze Uyaroğlu**	**Eren Meydan**
Presentation 5	Test Setup and Preperation	20	10	10

	Control of Experimental Setups	40	20	20
	Experimental Execution	10	0	10
	Data Processing and Interpretation	30	20	10
	Subtotal	**100**	**50**	**50**
	Total Work Contribution	**500**	**250**	**250**
Presentation Number	**Workpackages (WP)**	**Weight of WP**	**Gamze Uyaroğlu**	**Eren Meydan**
Presentation 6	Test Setup and Preperation	20	10	10
	Control of Experimental Setups	40	20	20
	Experimental Execution	10	10	0
	Data Processing and Interpretation	30	10	20
	Subtotal	**100**	**50**	**50**
	Total Work Contribution	**600**	**300**	**300**